Cure or Curse? Simulation Indicates that Microbes Proliferate under Disinfection Measures in the Space Station

Shuaishuai Li[1,2,5], Xiaolei Liu[1,2], Letian Chen[1,2], Hong Liu[1,2,3,4], Dawei Hu[1,2,3,4,]*

[1] School of Biological Science and Medical Engineering, Beihang University, Beijing 100083, China

[2] Institute of Environmental Biology and Life Support Technology, Beihang University, Beijing 100083, China

[3] International Joint Research Center of Aerospace Biotechnology and Medical Engineering, Beijing 100083, China

[4] State Key Laboratory of Virtual Reality Technology and Systems, School of Computer Science and Engineering, Beihang University, Beijing 100083, China

[5] Department of Biology, McGill University, Montréal, Québec, Canada H3A 1B1

* Corresponding author.

E-mail address: dwhu@163.com (D. Hu)

Postal address: 37 Xueyuan Road, Haidian District, Beijing, China

Abstract

The long-term stay on the space station requirement poses a knotty issue about the stable hardware and reliable guarantee of astronauts' health. Despite regular cleaning with wipes, microbes still proliferate in the space station. This study distilled three key factors—low-dose ionizing radiation, dilution and quaternary ammonium compound from the scenario. Species abundance and differential metabolites were applied to test their sole/combined influences on the three-simple-species microbial community succession. Mechanisms were built in mathematical models to generate the structural and behavior similarity with the phenomena. The results showed that LDIR, dilution and QAC, solely or jointly, could contribute to microbial proliferation. The synergy of

disturbances might convert them from harmful factors to rewarding ones (e.g. the transformation of QAC into nutrients under LDIR), leading to this "Ecological Surprise". These results shed light on the mechanisms driving microbial community succession in the space station and highlighted the need for tailored biocontrol strategies in the specific environment.

Keywords: microbial community succession, disturbance, low-dose ionizing radiation, dilution, quaternary ammonium compound(s).

Abbreviation:

LDIR: low-dose ionizing radiation; QAC: quaternary ammonium compound(s)

1. Introduction

Long-term residence on the space station needs stable hardware and guaranteed health status of astronauts (Brooks et al., 2014; Rosado et al., 2010; Sun et al., 2016; Yang et al., 2020), which is threatened by proliferative microbes on the inner surface of the space station (Alekhova et al., 2005). When the environmental factors are the same, the species diversity on the space station is much higher than that on the ground (Lang et al., 2017; Novikova et al., 2006), showing the phenomenon of the paradox of the plankton (G. E. Hutchinson, 1961; Yang et al., 2020). As astronauts and goods are the main sources of microbes in this closed environment (Lax et al., 2014; Singh et al., 2018), periodic cleaning is an actual plan for it. When carrying out the cleaning task, astronauts use wipes containing 0.1% quaternary ammonium compounds (QAC) (Singh et al., 2018) to wipe down the internal surface of the cabin under the low-dose ionizing radiation (LDIR) from the universe. However, the removal of microbes seems to be only effective for a short period of time and it is not complete. The microbes would

grow back after some time and the microbial community structure varies by time and location (Lang et al., 2017; Singh et al., 2018).

Understanding community succession mechanisms is always one of the core targets of ecology, especially microbial ecology(Powell et al., 2015; Stegen et al., 2013; Zhou & Ning, 2017). Disturbance, as a largely independent area of ecology, is the event that influences populations, resources or the physical environment in community succession (Pickett & White, 1985). Microbial removal by wiping, translated into the perspective of microbial community succession, is caused by abiotic environmental disturbance. This operation results in microscopic mass non-specific or specific death, macroscopic physical dilution and chemical disinfection events. Organisms are sensitive to the abiotic environment and community succession occurs when they are disturbed(Baudoin et al., 2008; Dangles & Chauvet, 2003; Tolkkinen et al., 2013). Although violent environmental degradation might lead to species extinction, some species could be favored under that circumstance because of the interactions necessary for survival in multi-species communities (Abreu et al., 2019, 2020). For example, evenly increasing mortality favors the faster grower, reversing the winner from the slower to the faster one in the competition (Hastings, 2013; Stewart & Levin, 1973). Nevertheless, current oversimplified models might lose some key information about the succession. Research to date has not yet determined how disturbances would work in resource-explicit models and the influence of selective disturbances.

In this study, three different types of disturbances, LDIR, dilution and QAC, were distilled from the scene of wiping the inner surface of the space station. Experiments with the simple three-species microbial community were carried out to demonstrate the species absolute abundance and differential metabolites in the community succession under different combinations and gradients of these disturbances. Results showed that

trends of community succession varied among different treatments and all types of disturbances could cause the proliferation of the community by the relief of competition or property transformation of specific chemicals. Afterward, some measures were proposed for microbe control in aerospace. Also, it is hoped that this research will contribute to a deeper understanding of community succession formations and mechanisms under different types of disturbances.

2. Materials and methods

2.1 Strains, culture and radiative environment simulation

Three laboratory-stored strains, *Bacillus subtilis* (CMCC(B) 63501), *Escherichia coli* (CMCC(B) 44102) and *Pseudomonas aeruginosa* (CMCC(B) 10104) were originally obtained from CMCC (China Medical Culture Collection). These three species were reported many times from microbial surveys in ISS, spacecrafts as well as related studies(Crabbé Aurélie et al., 2011; Singh et al., 2018; Urbaniak et al., 2018; Yang et al., 2021; Zea et al., 2016) and it was quite easy to distinguish them by genetic relationship.

To simulate the nutrient-deficient environment on the inner surface of the space station, the overnight cultures of the above strains were inoculated in the 10ml modified minimal R2A broth (Yang et al., 2021) with a total density of 1×10^6/ml calculated by direct counting under microscopy (Z. Song et al., 2015). The composition of modified minimal R2A was shown in Table S1. In the mixed culture, the initial ratio of three species was 1:1:1.

The LDIR environmental simulator (Fig. 1-A) was a refitted artificial climate chamber that simulated the LDIR environment in the space station. The modification included three main parts: a rotating wheel for placing the cultures, two X-ray tubes for alternatively ionizing the air inside to plasma, and a protective door for isolating the

radiation. Two X-ray tubes (XCH201, Dandong Shenbo Electronics Co. Ltd, China) were installed at the inside top of the chamber and run at 20kV, 0.2mA, alternately. To ensure that each culture is exposed to the same radiation dose, six boxes are affixed to the rotary wheel running at a constant angular velocity. These boxes contained plates with LDIR-treated cultures, while the control cultures without LDIR treatment were placed outside the radiation-exposed area but in the same climate chamber. The protective door was sealed to maintain a constant temperature of 30°C, and normal pressure during operation. The 3D geometric configuration of LDIR environmental simulator was accurately established using SolidWorks based on its int ernal dimensions, as shown in Fig. 1-B.

2.2 Periodic sampling and successive incubation

During a seven-day experiment cycle, 1ml samples were taken from cultures at the same time on each day. Then the residual parts were differently treated for successive incubation by distinct groups in Table 1. Each group contains three replicates. In each 1ml sample, 700μl was centrifuged for untargeted metabolomics test with its supernatant, and two portions of 90μl bacterial fluid were used to depict species abundance curves.

The composition of QAC was shown in Table 2.

2.3 Species abundance curve depicted by qPCR

Two portions of 90μl bacterial fluid above were applied to depict curves for *Bacillus subtilis* (Kirchhoff & Cypionka, 2017; Tut et al., 2021; Xie et al., 2016) by direct qPCR (Sup. A) and *Escherichia coli* as well as *Pseudomonas aeruginosa* by PMA-qPCR, separately.

For the PMA-treated one, 10μl 500mmol/L PMAxx (Cat. 40069, Biotium Inc., Hayward, CA, USA) was added into the sample under dark conditions for forming the

50mmol/L final concentration. Then the mixed solution was incubated at 20℃ for 40 min in the dark on a vortex with mild continuous shaking (100rpm) followed by the change of tube. Subsequently, the tube was exposure to a 120W blue LED light at 4℃ for 30 min (Agustí et al., 2018; Codony et al., 2020; Emerson et al., 2017; Fittipaldi et al., 2012; García-Fontana et al., 2016; Nocker et al., 2007) (Sup. B).

DNA was subsequently extracted from the solution above (with PMA or not) by direct boiling with glass beads (Li et al., 2023). 0.1g 0.1mm glass beads (Cat. 11079101, BioSpec Products, Inc., Bartlesville, OK, USA) were added into the tube containing 100μl resuspending solution before the heating procedure. After centrifugation, the supernatant is DNA solution.

The primers, their qPCR standard curves, their amplicons and the composition of qPCR reaction buffer were the same as our previous study (Li et al., 2023). 2×SYBR Green PCRmix (Cat. SR1110, Solarbio Science & Technology Co. Ltd., Beijing, China) was used to provide PCR Buffer, $MgCl_2$, dNTPs, Hs Taq DNA Polymerase, SYBR Green I and so on. Primers and standards of their amplicons (Banihashemi et al., 2012; Baymiev et al., 2020; Contreras et al., 2011; Emerson et al., 2017; Fittipaldi et al., 2012; Loozen et al., 2011; Martin et al., 2013; Schnetzinger et al., 2013) were commercially synthesized by Biomed Gene Technology Co., Ltd., Beijing, China. The reaction was performed using Gentier 96C real-time PCR system (Tianlong Science and Technology Co. Ltd., Xi'an, China). The qPCR amplification program included: pre-denaturation at 95°C for 10 min with a heating rate of 6°C/s; then 40 cycles of denaturation at 95°C for 10 sec with a temperature change rate of 5°C/s, annealing at 60°C for 20 sec with a cooling rate 5°C/s and elongation at 72°C for 30 sec with heating rate 6°C/s.

2.4 Untargeted metabolomics test

Metabolites were quantified using ultra-performance liquid chromatography-triple

quadrupole time-of-flight mass spectrometry (UPLC-MS) (Waters Corp., Milford, MA, USA). Raw data obtained from UPLC-MS were quantified in Progenesis QI (Waters Corp.). Significantly differential metabolites analysis was performed using BMKCloud (www.biocloud.net).

2.5 Mechanical modeling and computer simulation

The kinetic model of microbial community succession was established based on generalized Lotka-Volterra (gLV) equations and hypothetical mechanisms of disturbances. Parameters implying attributes in the community were embedded into the model and generated through computer Monte-Carlo experiments. Afterward, a corresponding simulation model with dde23 solver was established by S-Function of MATLAB/Simulink (MathWorks, Inc., Natick, MA, USA) to confirm the proposed hypothesis through behavior similarity between computer simulation and experimental data.

3. Results

This study aimed to demonstrate the influence of three different types of disturbances on microbial community succession. Experiments were taken to depict the species absolute abundance and differential metabolites during the succession. The following mechanical models and computer simulation were proposed to explain the mechanisms of phenomena in these experiments.

3.1 qPCR results

The overview of all conditions was shown in Fig. 2. As seen in this figure, distinct succession could be obtained by different treatments. Two-way repeated measured ANOVA was applied using R (4.0.2) to calculate the p-values to test if the curves showed a significant difference between the specific experimental group and the control group in the overall experimental period, where the interaction effect of treatment and

time was considered first. If the interaction effect was not significant, the main effect of treatment would be applied, where the p-value was marked as "p_m".

As shown in Fig. 3, in the control group, the total biomass and the absolute abundance of *E. coli* reached the highest points on the sixth day, when the density for both of them was about 1.5×10^{10}/ml.

When exposed to LDIR (Fig. 4), the microbial community thrived after a period of "hibernation". Compared with the control group, the total biomass rose on 5-7th days and still peaked on the 6th day, approximately reaching 3.5×10^{10}/ml. The majority was still *E. coli*. The abundance of *B. subtilis* showed the trend of damped periodic oscillations.

Dilution with gradients from 10% to 0.1‰ per day had no obvious different influence on the microbial community succession, as shown in Fig. S1 & S2. Taking 1‰ as an example (Fig. 5), compared with the control group, the total biomass and the abundance of *E. coli* decreased on 4-6th days, exhibiting the trend from oscillation to robustness. The abundance of *B. subtilis* significantly fell ($p_m = 1 \times 10^{-5}$), while that of *P. aeruginosa* rose dramatically ($p = 0.004$).

Imposing 100% and 10% stock solution of QAC could rapidly bring the total biomass down to below the initial density, when only *P. aeruginosa* could survive below the initial density under this condition (Fig. 2). However, 1% and 1‰ stock solution of QAC did not have the similar impact (Fig. 6). When treated with 1% stock solution of QAC, compared with the control group, the peak of total biomass moved back to 4th day, having no significant difference with the peak of the former. *E. coli* had a great contribution to the total biomass on the 1-4th days, followed by the sharp drop and extinction on the 6th day. Meanwhile, the abundance of *P. aeruginosa* increased from the 5th day and peaked on the 6th day. In the group of 1‰ treatment, the total

biomass exceeded the control group on the 7th day before the lag on the 4-6th days, presenting the trend of rise with fluctuations. The abundance of *E. coli* fluctuated continuously, and that of *P. aeruginosa* increased steadily.

When diluted with a 1‰ ratio per day, the total biomass ($p_m = 4 \times 10^{-4}$) and the abundance of *E. coli* ($p_m = 4 \times 10^{-4}$) significantly rose in the whole period of the LDIR group, compared with the group without LDIR (Fig. S3).

When exposed under LDIR, compared with the group without QAC, the total biomass of the 1% stock solution of QAC group increased on the 2-4th days but decreased on the 5-7th days, in which the abundance of *E. coli* went extinct quickly on the 5th day and that of *P. aeruginosa* peaked on 6th day (Fig. S4-A). The total biomass of the 1‰ stock solution of QAC group rose in fluctuations, exceeding the group without QAC on the 4th and 7th days but lagged on the 5-6th days, when the latter group was experiencing proliferation (Fig. S4-B). The majority was still *E. coli* but the magnitude of *P. aeruginosa* also improved.

When treated with 1% stock solution of QAC, the total biomass of the LDIR group went up in the whole period compared with the group without LDIR except on the 4th day, when the latter group peaked. The abundance of *E. coli* increased on 1-3rd days, then dropped on 4th day but this species still survived later. The abundance of *P. aeruginosa* rose during the whole period and still peaked on the 6th day (Fig. S5-A). When treated with 1‰ stock solution of QAC, the total biomass ($p = 0.003$) and the abundance of *E. coli* ($p = 0.02$) of the LDIR group dramatically rocketed with growing gaps in the whole period compared with the group without LDIR (Fig. S5-B). The abundance of *P. aeruginosa* shrank a little but the difference was not significant ($p > 0.05$).

When LDIR, 1‰ dilution and 1% stock solution of QAC were imposed, compared

with the control group (Fig. S6-A), *E. coli* went extinct quickly on the 2nd day. However, the abundance of *P. aeruginosa* substantially increased ($p = 3 \times 10^{-6}$). When LDIR, 1‰ dilution and 1‰ stock solution of QAC were imposed, compared with the control group (Fig. S6-B), the total biomass increased on 1-4th and 7th days, showing a trend of fluctuation. The abundance of *P. aeruginosa* markedly increased ($p = 3 \times 10^{-4}$).

3.2 Untargeted metabolomics test results

The samples involved in metabolite analysis were divided into 24 series according to biological repeat, and the symbol corresponding to the experimental condition of each group was shown in Table 3. The quality control, OPLS-DA as well as its validity test, OPLS-DA permutation test and screening of metabolites were done before analysis (Sup. C).

Compared with the control group, the concentration of p-coumaroyl agmatine in the group exposed under LDIR between 4-6th days dropped significantly ($p < 0.05$, Series B&M, C&N, D&O. Fig. S7). On 1st and 4-6th days, most of the metabolic pathways were inhibited, including polysaccharide metabolism, amino acid metabolism, vitamin metabolism, xenobiotic degradation and metabolism, as well as antibiotic biosynthesis (Series A&L, B&M, C&N, D&O; Fig. S8).

Compared with the control group, in the group diluted with 1‰ ratio per day, N-acetylmannosamine was enriched on the 4th day (Series B&F), which was markedly correlated with the rise of the abundance of *P. aeruginosa* ($p < 0.01$, Fig. S9). Pathways inhibited dominated on 4th day in the microbial community, including nucleotide metabolism, sugar degradation, antibiotic synthesis, and aminobenzoate degradation (Fig. S10).

When treated with 1% stock solution of QAC, N-acetylmannosamine was more abundant on 4th day compared with the control group (Series B&G), which was also

correlated with the rise of the abundance of *E. coli* ($p < 0.05$, Fig. S11). Meanwhile, staurosporine and tetracycline biosynthesis were active. When treated with 1‰ stock solution of QAC, echitovenine was rarer on the 7th day compared with the control group (Series E&K), which was also correlated with the increase of the abundance of *P. aeruginosa* ($p < 0.01$, Fig. S12). On the same day, aminobenzoate degradation as well as biosynthesis of alkaloids (derived from histidine and purine) were inhibited (Fig. S13).

When both LDIR and 1% stock solution of QAC were imposed, compared with the group under 1% stock solution of QAC, alkaloid biosynthesis was inhibited (Fig. S14), and some nitrogenous long-chain organic matters were enriched on 5-6th days (Series H&S, I&T), including tetradecenoyl carnitine and R-palmitoyl-(2-methyl) ethanolamide, ranging from $1 \times 10^{10} \sim 2 \times 10^{12}$ times; compared with the control group, cytochrome P450 metabolism was active on 5th day (Series C&S). When LDIR, 1‰ dilution and 1% stock solution of QAC were imposed together, the concentration of N-[(2R)-2-hydroxypropyl] hexadecanamide was 2×10^{12} times higher than the control group on the 4th day (Series B&W). However, when the QAC concentration was changed to 1‰ of the stock solution (Series B&V, B&X, E&W, J&V, K&W), the phenomenon of enrichment of nitrogenous long-chain organic matters disappeared; alternatively, cyanoamino acid metabolism, related to nitrogen metabolism (Ding et al., 2022), was active. The concentration of albaflavenone sharply diminished ($p < 0.01$, Fig. S15) on 4th day in the group with both LDIR and 1‰ stock solution of QAC, compared with the control group (Series B&V). Aminobenzoate degradation on the 4th day and antibiotic synthesis on the 7th day (Series K&W. Fig. S16) were restrained in the group with both LDIR and 1‰ stock solution of QAC, compared with 1‰ stock solution of QAC group. Under LDIR, when comparing 1% and 1‰ stock solution of

QAC groups, eicosanoids metabolism was active in the higher concentration one on the 4th day (Series R&V. Fig. S17).

3.3 Mechanical modeling and simulation results

3.3.1 State variables

The mechanical model was composed of six state variables in four types: *B. subtilis* biomass (x_1), *E. coli* biomass (x_2), *P.aeruginosa* biomass (x_3); amount of substrate (S), amount of QAC (Q), and amount of QAC degradation products (P).

3.3.2 Rate equations

(1) growth rate

The growth rate without competition of species i could be expressed as:

$$v_{ai} = \mu_i \left(\frac{S}{K_s + S}\right) x_i \tag{3.1}$$

where μ_i is the specific growth rate of species i, and K_s denotes substrate-dependent half-saturation constant for species i.

(2) interspecific competition

When there is no joint treatment of LDIR and QAC, the interspecific competition rate against species i could be written as follows:

$$v_{bi} = \sum_{j \neq i}^{3} \alpha_{ji} x_i \, x_j \tag{3.2}$$

where α_{ji} denotes the competition inhibition coefficient from species j to species i.

When the microbial community is treated with LDIR or QAC, the interspecific competition rate against species i could be written as follows:

$$v_{ci} = \sum_{j \neq i}^{3} \alpha_{ji} e^{-\left(c_{ji_R} R + c_{ji_Q} Q\right)} x_i \, x_j \tag{3.3}$$

Where I is a constant, representing the LDIR coefficient; e is the Euler number;

c_{ji_R} and c_{ji_Q} express the interspecies cross-feeding response coefficient between species j and species i caused by LDIR and QAC, respectively.

(3) intraspecific competition

When there is no joint treatment of LDIR and QAC, the intraspecific competition rate of species i could be written as follows:

$$v_{di} = \beta_i x_i^2 \tag{3.4}$$

where β_i denotes the intraspecific competition inhibition coefficient of species i.

When the microbial community is treated with LDIR or QAC, the intraspecific competition rate of species i could be written as follows:

$$v_{fi} = \beta_i e^{-(f_{i_R}R + f_{i_Q}Q)} x_i^2 \tag{3.5}$$

where, f_{i_R} and f_{i_Q} denote the intraspecies cross-feeding response coefficient of species i caused by LDIR and QAC, respectively.

(4) metabolism

The metabolism rate of species i could be expressed as:

$$v_{gi} = \delta_i x_i \tag{3.6}$$

where δ_i is the metabolism coefficient of species i.

(5) QAC disinfection

$$v_{hi} = \varepsilon_i Q x_i \tag{3.7}$$

where ε_i is the QAC disinfection rate on species i.

(6) QAC degradation

$$v_{mi} = \gamma RQ \tag{3.8}$$

where γ is the first-order kinetic coefficient of QAC degradation rate.

(7) generation of QAC degradation products

$$v_{ni} = \omega v_{mi} \tag{3.9}$$

where ω is the calibration coefficient.

(8) consumption of substrate

$$v_S = \sum_{i=1}^{3} \varphi_i \, v_{ai} \tag{3.10}$$

where φ_i is the substrate consumption coefficient during the growth of species i.

(9) transient influence of Dilution and QAC

a. only dilution

$$\begin{cases} S = S_0, t = 1,2, \dots, 7d \\ x_{i,t} = D x_{i,t-\Delta t} \end{cases} \tag{3.11}$$

where S_0 is the original substrate concentration of the R2A culture; $x_{i,t}$ is the abundance of species i at t moment; Δt is a very short time interval; D is the proportion of the culture just before dilution to the total volume.

b. only QAC

$$Q_t = Q_{t-\Delta t} + Q_{Add}, t = 1,2, \dots, 7d \tag{3.12}$$

where Q_{Add} denotes the QAC added.

c. both dilution and QAC

$$\begin{cases} S = S_0, t = 1,2, \dots, 7d \\ Q_t = D Q_{t-\Delta t} + Q_{Add}, t = 1,2, \dots, 7d \\ x_{i,t} = D x_{i,t-\Delta t} \end{cases} \tag{3.13}$$

3.3.3 the overall mechanical model

Based on Eq(3.1)~(3.13), the overall mechanical model, i.e. a state space model with six first-order nonlinear kinetic equations, could be formulated in a top-down manner as follows:

(1) When there is no joint treatment of LDIR and QAC, the population dynamics equation of species i is:

$$\frac{dx_i}{dt} = v_{ai} - v_{bi} - v_{di} - v_{gi} - v_{hi} = \mu_i \left(\frac{S}{K_s + S}\right) x_i - \sum_{j \neq i}^{3} \alpha_{ji} x_i \, x_j - \beta_i x_i^2 - \delta_i x_i - \varepsilon_i Q x_i \tag{3.14}$$

When there is joint treatment of LDIR and QAC, it is:

$$\frac{dx_i}{dt} = v_{ai} - v_{ci} - v_{fi} - v_{gi} - v_{hi} =$$

$$\mu_i\left(\frac{S}{K_s + S}\right)x_i - \sum_{j\neq i}^{3}\alpha_{ji}e^{-(c_{ji_R}R + c_{ji_Q}Q)}x_i\,x_j - \beta_i e^{-(f_{i_R}R + f_{i_Q}Q)}x_i^2 - \delta_i x_i - \varepsilon_i Q x_i \quad (3.15)$$

(2) The QAC degradation dynamics equation is:

$$\frac{dQ}{dt} = -v_{mi} = -\gamma RQ \quad (3.16)$$

(3) The generation of QAC degradation production dynamics equation is:

$$\frac{dP}{dt} = v_{ni} = \omega\gamma RQ \quad (3.17)$$

(4) The substrate change dynamics equation is:

$$\frac{dS}{dt} = v_{ni} - v_S = \omega\gamma RQ - \sum_{i=1}^{3}\varphi_i\,\mu_i\left(\frac{S}{K_s + S}\right)x_i \quad (3.18)$$

3.3.4 computer simulation

The code of the mechanical model above (Sup. D) was written by S-Function in MatLab/Simulink(R2019b, 9.7.0.1190202). The simulation experiments were implemented for simulating the control group and treatment groups of LDIR, dilution, QAC as well as their combinations, as shown in Fig. 7. The simulation results showed that the mechanical model had considerable behavior similarity with experiments, while the mathematical expression of the mechanical model matched the growth process of microbes, indicating the structure similarity between them. Therefore, the mechanical model was considered valid.

4. Discussion

In the present study, LDIR, dilution and QAC were extracted from the environment on the inner surface of the space station as treatments, and the microbial community succession under these uniformed different treatments was observed by measuring species abundance and metabolites. Mechanical models were built to explain the experiments, with which the computer simulation showed structural and behavioral similarity. The overall mechanisms are shown in Fig. 8.

At the later stage, LDIR improved the total biomass, every species abundance and their peaks, when the Hydra Effect happened. This phenomenon was shown in both with/without LDIR comparison and with/without LDIR comparison under dilution (Fig. 4 & S3). The p-coumaroylagmatine could thicken cell walls, limit bacterial movement and improve plant defense against pathogens(Häusler et al., 2014; Macoy et al., 2015), thus its decrease on the 4-6th days (Series B&M, C&N, D&O) indicated that the physiological activity of the microbial community was enhanced under LDIR. The inhibited antibiotic synthesis pathway (Series B&M) suggested that external pressure was reduced and interspecific competition was diminished. Therefore, the Hydra Effect occurred under LDIR. This effect was more significant as the main effect in the comparison of the group under LDIR and 1‰ dilution and only 1‰ dilution (Fig. S3). Except in *P. aeruginosa*, dilution reshuffled all other components everyday and undermined the interaction effect of treatment and time, where the enhancement effect of LDIR emerged.

Dilution, by removing a certain part of biomass during serial transfers, was a non-specific and highly controllable disturbance way, where the transient removal did not depend on response traits in the microbial community (Gibbons et al., 2016). However, under non-selective dilution, *P. aeruginosa* was selectively released from competitive exclusion. Aminobenzoate was the signal of xenobiotic degradation (Patil et al., 2020; Wang et al., 2020), thus its degradation inhibition on 4th day (Series B&F) suggested that organisms tended not to consume energy storage material (Smitha et al., 2017) and the competition in the community was mitigated. It could be inferred that many niches would be released without distinction under dilution, when *P. aeruginosa* could reproduce based on its merits beyond others' (Abreu et al., 2019) and occupy these niches. This release happened only under dilution with all gradients; when both dilution

and LDIR were applied, *E.coli* took the majority again (Fig. S18-A).

QAC stood for specific disturbances, causing non-random removal according to the microbe's response traits(Banitz et al., 2020; Calderón et al., 2018; Jurburg et al., 2017; Srivastava & Vellend, 2005). Its effect also counted on the disturbance intensities and frequencies. Different QAC concentrations had various influences on the microbial community, from elimination to promotion. The Hydra Effect even happened under 1% and 1‰ stock solution of QAC, where simple competition mitigation cannot explain. Polymers of N-acetylmannosamine played a protective role in *E. coli* (Sellner et al., 2021), thus their respective increments with dramatical correlation told the reason why the species abundance of *E. coli* peaked in advance on the 4th day under 1% stock solution (Series B&G). Besides, the active biosynthetic pathways of antibiotics and cytokinins on the same day corroborated that microbes combated adversity by more cell division and the total biomass also peaked. Echitovenine was a monoterpene alkaloid with antimicrobial activity (Mohammed et al., 2021), whose attenuation could interpret the growth of *P. aeruginosa* on the 7th day under 1‰ stock solution (Series E&K), given their notable correlation. QAC would periodically selectively remove a portion of individuals in the community, leading the way of community succession to the direction of dominance by species that can tolerate the environment, which could be pronounced in comparisons across gradients (Figure S18-B&C). With low-concentration QAC treatment, the community had adapted to the environment and utilized it. QAC, was a series of long-chain organics that could be used by microbes, especially in microbial co-metabolism by *Pseudomonas* (Harris & Knowles, 1983; Leadbetter & Foster, 1960; Zhang et al., 2015), which was widely and systemically utilized in treating wastewater (biological nitrogen removal). On the oligotrophic surface of the space station, the carbon sources were mostly wiped down, when co-

metabolism might allow microbes to survive with remaining nitrogen sources. Meanwhile, the inhibition of aminobenzoate degradation pathway also flanked the corresponding decrease of the consumption of energy storage in the community.

The upsurge of some nitrogenous long-chain organic matters under both LDIR and QAC, compared with only QAC or the control group, strongly implies that QAC may undergo radiolysis under LDIR. Several studies (Baidak & LaVerne, 2010; Dhiman & LaVerne, 2013; Nogami et al., 1996; Pillay, 1986) implied that radiolysis would happen on substrates containing QAC, especially under water acceleration. 1% stock solution of QAC is substantially transformed from the toxic bactericide to organic nitrogenous long-chain nutrients, including tetradecenoyl carnitine, R-palmitoyl-(2-methyl) ethanolamide and N-[(2R)-2-hydroxypropyl] hexadecanamide with significant differences between Series B&W, H&S, I&T. This might accelerate the microbial co-metabolism process. Cytochrome P450-related enzymes prefer long-chain fatty acids with 15-16 carbon atoms (Lewis & Wiseman, 2005), thus its activation might be related to added long-chain QAC utilization. Inhibited alkaloid biosynthesis (Series H&S, I&T) and ameliorated cytochrome P450 metabolism (Series C&S) also shows that the community could adapt to and consume QAC under LDIR. Nevertheless, when the QAC concentration is 1‰, significant differences are no longer detected for organic nitrogenous long-chain nutrients (Series B&V, B&X, E&W, J&V, K&W), suggesting that the community can entirely co-metabolize QAC in this situation. The activation of cyanoamino acid metabolism (Series B&X), inhibition of aminobenzoate degradation (Series J&V) as well as inhibition of antibiotic synthesis (Series K&W) also reconfirm the speculation of utilization of exogenous QAC as the source of nitrogen and less pressure of the community caused by LDIR. Comparing different concentration of QAC under LDIR (Series V&R), the active eicosanoids metabolism in the higher

concentration one shows that the microbes might transform QAC into long-chain fatty acid substances for consuming.

The proliferative microbes on the inner surface of the space station (Alekhova et al., 2005) have been threatening its normal operation, which is a serious problem and could be shifted to the issue of the effect of disturbance on community succession. Disturbance is acknowledged as a key factor of biodiversity via affecting eco-processes (Banitz et al., 2020). However, the mechanisms behind the observed community diversity under disturbance need to be further clarified (Fox, 2013; Shea et al., 2004). First, few quantitative studies on disturbances have been reported, while more relative studies focus on the qualitative aspect — this is due to both the difficulty in defining the attribute of frequency, intensity, as well as extent (Shade et al., 2012), and the wide variety of their characteristics and ecological impacts (Fraterrigo & Rusak, 2008). Second, few studies are explicitly based on the time course of microbial community composition under disturbance; instead, many solely studies are on the sensitivity of composition at a given moment (Allison & Martiny, 2008), which is attributed to the inertial thinking in community ecology and research tools in microbiology. Our previous study noticed the benefit of sole LDIR for the microbial community (Yang et al., 2021). Abreu et al. (Abreu et al., 2019, 2020) expanded the effect of dilution on multispecies community composition, providing an example for quantifying disturbances with the time course. Nonetheless, in their research, when distinguishing disturbances by pulsed versus sustained, pulsed ones like dilution are not applicable for being directly integrated into the typical LV equation. Finally, studies with similar gradient-based methods on combined multiple factors with synergy, are still at an early stage. Most studies still concentrate on a single factor, and only a few have noticed the combined influence of multiple factors (Banitz et al., 2020; Zeng et al., 2020). In

contrast, a large number of phenomena in nature are caused by the complex interaction of the latter condition (Elmqvist et al., 2003; Martínez-Ramos et al., 2016), including "ecological surprises" such as drastic shifts in community compositions and biodiversity (Banitz et al., 2020; Filbee-Dexter et al., 2017; Newman, 2019).

In this study, "ecological surprise" occurred when human expectations deviated from the observed community succession behavior (Doak et al., 2008; Filbee-Dexter et al., 2017). And these unexpected dynamics arose from human management and disturbances (Doak et al., 2008). Dilution (wiping) and QAC were recognized as efficient measures to take control of microbes (Sattar et al., 2015; Zhang et al., 2015) and applied in the space station (Singh et al., 2018). However, given the results above, the synergy emerged between LDIR and QAC, thus low-concentration QAC was transformed from the bactericide to nitrogen-rich long-chain nutrients. Selectively released *P. aeruginosa* under suppression after dilution would take these nutrients to thrive, changing the community structure and dominant species. That could be a possible reason for the phenomenon in the space station, and also gave a potential mechanism for "ecological surprise" under synergistical disturbances. It reminded us that tailored biocontrol strategies ought to be considered for the specific environment. Sometimes, the control measures were taken for granted that they were "disturbances" affecting the targets without the consideration of their own properties and changes. It cannot be neglected that general strategies might not function under certain conditions.

Given the current microbial prevention strategies have some disadvantages, future improvements can be adopted. Concerning the low concentration of QAC, except for co-metabolism and radiolysis of QAC mentioned above, the pre-package of wipes can also cause it by both reduced antimicrobial activity of QAC with a long-term soaking (Bloß et al., 2010, 2010; Slopek et al., 2011) and the chemical combination with the

wipe fibre (Dharan et al., 1999; X. Song et al., 2019). The target surface properties also influence the disinfection (X. Song et al., 2019). More organic contamination on (dirtier) the surface, lower the disinfection effect (Williams et al., 2007). Moreover, radiolysis could happen just after the spacecraft entered the outer space. In terms of dilution, its rate was limited on the order of 1% even using two wipes successively (Gold & Hitchins, 2013), which is not enough given the results in this study. Furthermore, “wiping” itself could lead to cross-contamination of microorganisms in different locations by mechanical stimulation (Ramm et al., 2015; Siani et al., 2011; Williams et al., 2007). To attenuate these effects, several measures could be considered. Such as augmenting local wiping time, wiping with mechanical equipment to restraint power variation (Sattar et al., 2015; Williams et al., 2007), special antibacterial treatment on the surface requiring microbial prevention, applying different wipe materials harder to react with QAC, adjusting the formulation of QAC for a lower degradation rate (Pillay, 1986; Zhang et al., 2015), avoiding surface exposure to radiation after wiping.

Despite these promising results, questions still remain. Further work is needed to develop reliable experimental and analytical methods (e.g. based on the individual-based model) (Li et al., 2022) for testing community succession considering the spatial factor. The liquid culture implemented in this study aborted it because of current biotechnology limitations on detecting microbial individuals. Additional research based on more methods in bioinformatics is needed to better understand the successive changes in microbial behaviors under disturbances. This study focused on the level of community succession. Hence, there is abundant room for further progress in determining the evolutionary characteristics changes of the species facing disturbances in long-term experiments.

5. Conclusion

In this study, the intricate relationship between disturbance and the microbial community succession in the space station was elucidated. The proliferation under LDIR, the selective species release under dilution and complex responses of the community to QAC concentration were observed in experiments and their similarity was tested in modeling. The synergy of combined disturbances, QAC and LDIR, led to the transformation of them from harmful factors to supportive ones. Therefore, it is necessary to consider synergistic effects and to apply tailored strategies when addressing the microbial proliferation challenge as well as other similar circumstances.

Fundings

This study was financially supported by Funds for International Cooperation and Exchange of the National Natural Science Foundation of China (32261133528).

Acknowledgment

We sincerely acknowledge the assistance from Chuanmeng Cai, Dengbo Chen, and Yong Feng in the long and non-stop periodic experiment, and the assistance from Yong Feng for depicting Fig.1-B.

References

Abreu, C. I., Andersen Woltz, V. L., Friedman, J., & Gore, J. (2020). Microbial communities display alternative stable states in a fluctuating environment. *PLOS Computational Biology*, *16*(5), e1007934. https://doi.org/10.1371/journal.pcbi.1007934

Abreu, C. I., Friedman, J., Andersen Woltz, V. L., & Gore, J. (2019). Mortality causes universal changes in microbial community composition. *Nature Communications*, *10*(1), 2120. https://doi.org/10.1038/s41467-019-09925-0

Agustí, G., Fittipaldi, M., & Codony, F. (2018). Optimization of a Viability PCR Method for the Detection of Listeria monocytogenes in Food Samples. *Current Microbiology*, *75*(6), 779–785. https://doi.org/10.1007/s00284-018-1448-6

Alekhova, T. A., Aleksandrova, A. A., Novozhilova, T. Y., Lysak, L. V., Zagustina, N. A., & Bezborodov, A. M. (2005). Monitoring of Microbial Degraders in Manned Space Stations. *Applied Biochemistry and Microbiology*, *41*(4), 382–389. https://doi.org/10.1007/s10438-005-0065-x

Allison, S. D., & Martiny, J. B. H. (2008). Resistance, resilience, and redundancy in microbial communities. *Proceedings of the National Academy of Sciences*, *105*(Supplement 1), 11512–11519. https://doi.org/10.1073/pnas.0801925105

Baidak, A., & LaVerne, J. A. (2010). Radiation-induced decomposition of anion exchange resins. *Journal of Nuclear Materials*, *407*(3), 211–219. https://doi.org/10.1016/j.jnucmat.2010.10.025

Banihashemi, A., Dyke, M. I., & Huck, P. M. (2012). Long-amplicon propidium monoazide-PCR enumeration assay to detect viable Campylobacter and Salmonella. *Journal of Applied Microbiology*, *113*(4), 863–873. https://doi.org/10.1111/j.1365-2672.2012.05382.x

Banitz, T., Chatzinotas, A., & Worrich, A. (2020). Prospects for Integrating Disturbances, Biodiversity and Ecosystem Functioning Using Microbial Systems. *Frontiers in Ecology and Evolution*, *8*. https://www.frontiersin.org/articles/10.3389/fevo.2020.00021

Baudoin, J. M., Guérold, F., Felten, V., Chauvet, E., Wagner, P., & Rousselle, P. (2008). Elevated Aluminium Concentration in Acidified Headwater Streams Lowers Aquatic Hyphomycete Diversity and Impairs Leaf-Litter Breakdown. *Microbial Ecology*, *56*(2), 260–269. https://doi.org/10.1007/s00248-007-9344-9

Baymiev, An. Kh., Baymiev, Al. Kh., Kuluev, B. R., Shvets, K. Yu., Yamidanov, R. S., Matniyazov, R. T., Chemeris, D. A., Zubov, V. V., Alekseev, Ya. I., Mavzyutov, A. R., Ivanenkov, Ya. A., & Chemeris, A. V. (2020). Modern Approaches to Differentiation of Live and Dead Bacteria Using Selective Amplification of Nucleic Acids. *Microbiology*, *89*(1), 13–27. https://doi.org/10.1134/S0026261720010038

Bloß, R., Meyer, S., & Kampf, G. (2010). Adsorption of active ingredients of surface disinfectants depends on the type of fabric used for surface treatment. *Journal of Hospital Infection*, *75*(1), 56–61. https://doi.org/10.1016/j.jhin.2009.11.027

Brooks, B., Firek, B. A., Miller, C. S., Sharon, I., Thomas, B. C., Baker, R., Morowitz, M. J., & Banfield, J. F. (2014). Microbes in the neonatal intensive care unit resemble those found in the gut of premature infants. *Microbiome*, *2*(1), 1. https://doi.org/10.1186/2049-2618-2-1

Calderón, K., Philippot, L., Bizouard, F., Breuil, M.-C., Bru, D., & Spor, A. (2018). Compounded Disturbance Chronology Modulates the Resilience of Soil Microbial Communities and N-Cycle Related Functions. *Frontiers in Microbiology*, *9*, 2721. https://doi.org/10.3389/fmicb.2018.02721

Codony, F., Dinh-Thanh, M., & Agustí, G. (2020). Key Factors for Removing Bias in Viability PCR-Based Methods: A Review. *Current Microbiology*, *77*(4), 682–687. https://doi.org/10.1007/s00284-019-01829-y

Contreras, P. J., Urrutia, H., Sossa, K., & Nocker, A. (2011). Effect of PCR amplicon length on suppressing signals from membrane-compromised cells by propidium monoazide treatment. *Journal of Microbiological Methods*, *87*(1), 89–95. https://doi.org/10.1016/j.mimet.2011.07.016

Crabbé Aurélie, Schurr Michael J., Monsieurs Pieter, Morici Lisa, Schurr Jill, Wilson James W., Ott C. Mark, Tsaprailis George, Pierson Duane L., Stefanyshyn-Piper Heidi, & Nickerson Cheryl A. (2011). Transcriptional and Proteomic Responses of Pseudomonas aeruginosa PAO1 to Spaceflight Conditions Involve Hfq Regulation and Reveal a Role for Oxygen. *Applied and Environmental Microbiology*, *77*(4), 1221–1230. https://doi.org/10.1128/AEM.01582-10

Dangles, O., & Chauvet, E. (2003). Effects of stream acidification on fungal biomass in decaying beech leaves and leaf palatability. *Water Research*, *37*(3), 533–538. https://doi.org/10.1016/S0043-1354(02)00359-7

Dharan, S., Mourouga, P., Copin, P., Bessmer, G., Tschanz, B., & Pittet, D. (1999). Routine disinfection of patients' environmental surfaces. Myth or reality? *Journal of Hospital Infection*, *42*(2), 113–117. https://doi.org/10.1053/jhin.1999.0567

Dhiman, S. B., & LaVerne, J. A. (2013). Radiolysis of simple quaternary ammonium salt components of Amberlite resin. *Journal of Nuclear Materials*, *436*(1–3), 8–13. https://doi.org/10.1016/j.jnucmat.2013.01.294

Ding, C., Wang, S., Li, J., & Wang, Z. (2022). Transcriptomic analysis reveals the mechanism of host growth promotion by endophytic fungus of Rumex gmelinii Turcz. *Archives of Microbiology*, *204*(7), 1–13.

Doak, D. F., Estes, J. A., Halpern, B. S., Jacob, U., Lindberg, D. R., Lovvorn, J., Monson, D. H., Tinker, M. T., Williams, T. M., Wootton, J. T., & others. (2008). Understanding and predicting ecological dynamics: Are major surprises inevitable. *Ecology*, *89*(4), 952–961.

Elmqvist, T., Folke, C., Nyström, M., Peterson, G., Bengtsson, J., Walker, B., & Norberg, J. (2003). Response diversity, ecosystem change, and resilience. *Frontiers in Ecology and the Environment*, *1*(9), 488–494. https://doi.org/10.1890/1540-9295(2003)001[0488:RDECAR]2.0.CO;2

Emerson, J. B., Adams, R. I., Román, C. M. B., Brooks, B., Coil, D. A., Dahlhausen, K., Ganz, H. H., Hartmann, E. M., Hsu, T., Justice, N. B., Paulino-Lima, I. G., Luongo, J. C., Lymperopoulou, D. S., Gomez-Silvan, C., Rothschild-Mancinelli, B., Balk, M., Huttenhower, C., Nocker, A., Vaishampayan, P., & Rothschild, L. J. (2017). Schrödinger's microbes: Tools for distinguishing the living from the dead in microbial ecosystems. *Microbiome*, *5*(1), 86. https://doi.org/10.1186/s40168-017-0285-3

Filbee-Dexter, K., Pittman, J., Haig, H. A., Alexander, S. M., Symons, C. C., & Burke, M. J. (2017). Ecological surprise: Concept, synthesis, and social dimensions. *Ecosphere*, *8*(12), e02005. https://doi.org/10.1002/ecs2.2005

Fittipaldi, M., Nocker, A., & Codony, F. (2012). Progress in understanding preferential detection of live cells using viability dyes in combination with DNA amplification. *Journal of Microbiological Methods*, *91*(2), 276–289. https://doi.org/10.1016/j.mimet.2012.08.007

Fleischmann, S., Robben, C., Alter, T., Rossmanith, P., & Mester, P. (2021). How to Evaluate Non-Growing Cells—Current Strategies for Determining Antimicrobial Resistance of VBNC Bacteria. *Antibiotics*, *10*(2), 115. https://doi.org/10.3390/antibiotics10020115

Fox, J. W. (2013). The intermediate disturbance hypothesis is broadly defined, substantive issues are key: A reply to Sheil and Burslem. *Trends in Ecology & Evolution*, *28*(10), 572–573. https://doi.org/10.1016/j.tree.2013.07.008

Fraterrigo, J. M., & Rusak, J. A. (2008). Disturbance-driven changes in the variability of ecological patterns and processes. *Ecology Letters*, *11*(7), 756–770. https://doi.org/10.1111/j.1461-0248.2008.01191.x

G. E. Hutchinson. (1961). The Paradox of the Plankton. *The American Naturalist*, *95*(882), 137–145.

García-Fontana, C., Narváez-Reinaldo, J. J., Castillo, F., González-López, J., Luque, I., & Manzanera, M. (2016). A New Physiological Role for the DNA Molecule as a Protector against Drying Stress in Desiccation-Tolerant Microorganisms. *Frontiers in Microbiology*, *7*. https://doi.org/10.3389/fmicb.2016.02066

Gibbons, S. M., Scholz, M., Hutchison, A. L., Dinner, A. R., Gilbert, J. A., & Coleman, M. L. (2016). Disturbance Regimes Predictably Alter Diversity in an Ecologically Complex Bacterial System. *mBio*, *7*(6). https://doi.org/10.1128/mBio.01372-16

Gold, K. M., & Hitchins, V. M. (2013). Cleaning assessment of disinfectant cleaning wipes on an external surface of a medical device contaminated with artificial blood or *Streptococcus pneumoniae*. *American Journal of Infection Control*, *41*(10), 901–907. https://doi.org/10.1016/j.ajic.2013.01.029

Harris, R., & Knowles, C. J. (1983). Isolation and Growth of a Pseudomonas Species that Utilizes Cyanide as a Source of Nitrogen. In *Microbiology* (Vol. 129, Issue 4, pp. 1005–1011). Microbiology Society. https://doi.org/10.1099/00221287-129-4-1005

Hastings, A. (2013). *Population biology: Concepts and models*. Springer Science & Business Media.

Häusler, R. E., Ludewig, F., & Krueger, S. (2014). Amino acids – A life between metabolism and signaling. *Plant Science*, *229*, 225–237. https://doi.org/10.1016/j.plantsci.2014.09.011

Jurburg, S. D., Nunes, I., Brejnrod, A., Jacquiod, S., Priemé, A., Sørensen, S. J., Van Elsas, J. D., & Salles, J. F. (2017). Legacy Effects on the Recovery of Soil Bacterial Communities from Extreme Temperature Perturbation. *Frontiers in Microbiology*, *8*, 1832. https://doi.org/10.3389/fmicb.2017.01832

Kirchhoff, C., & Cypionka, H. (2017). Propidium ion enters viable cells with high membrane potential during live-dead staining. *Journal of Microbiological Methods*, *142*, 79–82. https://doi.org/10.1016/j.mimet.2017.09.011

Kralik, P., Nocker, A., & Pavlik, I. (2010). Mycobacterium avium subsp. Paratuberculosis viability determination using F57 quantitative PCR in combination with propidium monoazide treatment. *International Journal of Food Microbiology*, *141*, S80–S86. https://doi.org/10.1016/j.ijfoodmicro.2010.03.018

Lang, J. M., Coil, D. A., Neches, R. Y., Brown, W. E., Cavalier, D., Severance, M., Hampton-Marcell, J. T., Gilbert, J. A., & Eisen, J. A. (2017). A microbial survey of the International Space Station (ISS). *PeerJ*, *5*, e4029. https://doi.org/10.7717/peerj.4029

Lax, S., Smith, D. P., Hampton-Marcell, J., Owens, S. M., Handley, K. M., Scott, N. M., Gibbons, S. M., Larsen, P., Shogan, B. D., Weiss, S., Metcalf, J. L., Ursell, L. K., Vázquez-Baeza, Y., Van Treuren, W., Hasan, N. A., Gibson, M. K., Colwell, R., Dantas, G., Knight, R., & Gilbert, J. A. (2014). Longitudinal analysis of microbial interaction between humans and the indoor environment. *Science*, *345*(6200), 1048–1052. https://doi.org/10.1126/science.1254529

Leadbetter, E. R., & Foster, J. W. (1960). Bacterial oxidation of gaseous alkanes. *Archiv Für Mikrobiologie*, *35*(1), 92–104. https://doi.org/10.1007/BF00425597

Lewis, D. F. V., & Wiseman, A. (2005). A selective review of bacterial forms of cytochrome P450 enzymes. *Enzyme and Microbial Technology*, *36*(4), 377–384. https://doi.org/10.1016/j.enzmictec.2004.07.018

Li, S., Liu, H., Liu, G., & Hu, D. (2022). Simulated artificial interventions maintain species diversity of spatially structured microbial communities in closed ecosystem. *Acta Astronautica*, *201*, 39–47. https://doi.org/10.1016/j.actaastro.2022.08.023

Li, S., Liu, X., Li, Z., Liu, H., & Hu, D. (2023). Combination of direct boiling and glass beads increases the purity and accuracy of bacterial DNA extraction. *Biotechnology Journal*, *18*(11), 2300135.

Loozen, G., Boon, N., Pauwels, M., Quirynen, M., & Teughels, W. (2011). Live/dead real-time polymerase chain reaction to assess new therapies against dental plaque-related pathologies: Vitality real-time PCR. *Molecular Oral Microbiology*, *26*(4), 253–261. https://doi.org/10.1111/j.2041-1014.2011.00615.x

Macoy, D. M., Kim, W.-Y., Lee, S. Y., & Kim, M. G. (2015). Biotic stress related functions of hydroxycinnamic acid amide in plants. *Journal of Plant Biology*, *58*(3), 156–163.

https://doi.org/10.1007/s12374-015-0104-y

Martin, B., Raurich, S., Garriga, M., & Aymerich, T. (2013). Effect of Amplicon Length in Propidium Monoazide Quantitative PCR for the Enumeration of Viable Cells of Salmonella in Cooked Ham. *Food Analytical Methods*, *6*(2), 683–690. https://doi.org/10.1007/s12161-012-9460-0

Martínez-Ramos, M., Ortiz-Rodríguez, I. A., Piñero, D., Dirzo, R., & Sarukhán, J. (2016). Anthropogenic disturbances jeopardize biodiversity conservation within tropical rainforest reserves. *Proceedings of the National Academy of Sciences*, *113*(19), 5323–5328. https://doi.org/10.1073/pnas.1602893113

Mohammed, A. E., Abdul-Hameed, Z. H., Alotaibi, M. O., Bawakid, N. O., Sobahi, T. R., Abdel-Lateff, A., & Alarif, W. M. (2021). Chemical Diversity and Bioactivities of Monoterpene Indole Alkaloids (MIAs) from Six Apocynaceae Genera. *Molecules*, *26*(2), 488. https://doi.org/10.3390/molecules26020488

Newman, E. A. (2019). Disturbance Ecology in the Anthropocene. *Frontiers in Ecology and Evolution*, *7*, 147. https://doi.org/10.3389/fevo.2019.00147

Nocker, A., Sossa, K. E., & Camper, A. K. (2007). Molecular monitoring of disinfection efficacy using propidium monoazide in combination with quantitative PCR. *Journal of Microbiological Methods*, *70*(2), 252–260. https://doi.org/10.1016/j.mimet.2007.04.014

Nogami, M., Fujii, Y., & Sugo, T. (1996). Radiation resistance of pyridine type anion exchange resins for spent fuel treatment. *Journal of Radioanalytical and Nuclear Chemistry Articles*, *203*(1), 109–117. https://doi.org/10.1007/BF02060385

Novikova, N., De Boever, P., Poddubko, S., Deshevaya, E., Polikarpov, N., Rakova, N., Coninx, I., & Mergeay, M. (2006). Survey of environmental biocontamination on board the International Space Station. *Research in Microbiology*, *157*(1), 5–12. https://doi.org/10.1016/j.resmic.2005.07.010

Patil, S. M., Suryavanshi, M. V., Chandanshive, V. V., Kurade, M. B., Govindwar, S. P., & Jeon, B.-H. (2020). Regeneration of textile wastewater deteriorated microbial diversity of soil microcosm through bioaugmentation. *Chemical Engineering Journal*, *380*, 122533. https://doi.org/10.1016/j.cej.2019.122533

Pickett, S., & White, P. (1985). *Ecology of natural disturbance and patch dynamics*.

Pillay, K. K. S. (1986). A review of the radiation stability of ion exchange materials. *Journal of Radioanalytical and Nuclear Chemistry Articles*, *102*(1), 247–268. https://doi.org/10.1007/BF02037966

Powell, J. R., Karunaratne, S., Campbell, C. D., Yao, H., Robinson, L., & Singh, B. K. (2015). Deterministic processes vary during community assembly for ecologically dissimilar taxa. *Nature Communications*, *6*(1), 8444. https://doi.org/10.1038/ncomms9444

Ramm, L., Siani, H., Wesgate, R., & Maillard, J.-Y. (2015). Pathogen transfer and high variability in pathogen removal by detergent wipes. *American Journal of Infection Control*, *43*(7), 724–

728. https://doi.org/10.1016/j.ajic.2015.03.024

Rosado, H., Doyle, M., Hinds, J., & Taylor, P. W. (2010). Low-shear modelled microgravity alters expression of virulence determinants of Staphylococcus aureus. *Acta Astronautica*, *66*(3), 408–413. https://doi.org/10.1016/j.actaastro.2009.06.007

Sattar, S. A., Bradley, C., Kibbee, R., Wesgate, R., Wilkinson, M. A. C., Sharpe, T., & Maillard, J.-Y. (2015). Disinfectant wipes are appropriate to control microbial bioburden from surfaces: Use of a new ASTM standard test protocol to demonstrate efficacy. *Journal of Hospital Infection*, *91*(4), 319–325. https://doi.org/10.1016/j.jhin.2015.08.026

Schnetzinger, F., Pan, Y., & Nocker, A. (2013). Use of propidium monoazide and increased amplicon length reduce false-positive signals in quantitative PCR for bioburden analysis. *Applied Microbiology and Biotechnology*, *97*(5), 2153–2162. https://doi.org/10.1007/s00253-013-4711-6

Sellner, B., Prakapaitė, R., van Berkum, M., Heinemann, M., Harms, A., & Jenal, U. (2021). A New Sugar for an Old Phage: A c-di-GMP-Dependent Polysaccharide Pathway Sensitizes *Escherichia coli* for Bacteriophage Infection. *mBio*, *12*(6), e03246-21. https://doi.org/10.1128/mbio.03246-21

Shade, A., Peter, H., Allison, S. D., Baho, D. L., Berga, M., Bürgmann, H., Huber, D. H., Langenheder, S., Lennon, J. T., Martiny, J. B., & others. (2012). Fundamentals of microbial community resistance and resilience. *Frontiers in Microbiology*, *3*, 417.

Shea, K., Roxburgh, S. H., & Rauschert, E. S. J. (2004). Moving from pattern to process: Coexistence mechanisms under intermediate disturbance regimes. *Ecology Letters*, *7*(6), 491–508. https://doi.org/10.1111/j.1461-0248.2004.00600.x

Siani, H., Cooper, C., & Maillard, J.-Y. (2011). Efficacy of "sporicidal" wipes against Clostridium difficile. *American Journal of Infection Control*, *39*(3), 212–218. https://doi.org/10.1016/j.ajic.2011.01.006

Singh, N. K., Wood, J. M., Karouia, F., & Venkateswaran, K. (2018). Succession and persistence of microbial communities and antimicrobial resistance genes associated with International Space Station environmental surfaces. *Microbiome*, *6*(1), 204. https://doi.org/10.1186/s40168-018-0585-2

Slopek, R., Condon, B., Sawhney, P., Reynolds, M., & Allen, C. (2011). Adsorption of alkyl-dimethyl-benzyl-ammonium chloride on differently pretreated non-woven cotton substrates. *Textile Research Journal*, *81*(15), 1617–1624. https://doi.org/10.1177/0040517511407373

Smitha, M., Singh, S., & Singh, R. (2017). Microbial biotransformation: A process for chemical alterations. *J Bacteriol Mycol Open Access*, *4*(2), 85.

Song, X., Vossebein, L., & Zille, A. (2019). Efficacy of disinfectant-impregnated wipes used for surface disinfection in hospitals: A review. *Antimicrobial Resistance & Infection Control*, *8*(1), 139. https://doi.org/10.1186/s13756-019-0595-2

Song, Z., Han, H., & Zhu, W. (2015). Morphological variation and recovery mechanism of residual

crude oil by biosurfactant from indigenous bacteria: Macro-and pore-scale experimental investigations. *Journal of Microbiology and Biotechnology*, *25*(6), 918–929.

Srivastava, D. S., & Vellend, M. (2005). Biodiversity-Ecosystem Function Research: Is It Relevant to Conservation? *Annual Review of Ecology, Evolution, and Systematics*, *36*(1), 267–294. https://doi.org/10.1146/annurev.ecolsys.36.102003.152636

Stegen, J. C., Lin, X., Fredrickson, J. K., Chen, X., Kennedy, D. W., Murray, C. J., Rockhold, M. L., & Konopka, A. (2013). Quantifying community assembly processes and identifying features that impose them. *The ISME Journal*, *7*(11), 2069–2079. https://doi.org/10.1038/ismej.2013.93

Stewart, F. M., & Levin, B. R. (1973). Partitioning of Resources and the Outcome of Interspecific Competition: A Model and Some General Considerations. *The American Naturalist*, *107*(954), 171–198. https://doi.org/10.1086/282825

Sun, Y., Hu, D., Li, L., Jing, Z., Wei, C., Zhang, L., Fu, Y., & Liu, H. (2016). Influence mechanism of low-dose ionizing radiation on Escherichia coli DH5α population based on plasma theory and system dynamics simulation. *Journal of Environmental Radioactivity*, *151*, 185–192. https://doi.org/10.1016/j.jenvrad.2015.10.007

Tolkkinen, M., Mykrä, H., Markkola, A., Aisala, H., Vuori, K., Lumme, J., Pirttilä, A. M., & Muotka, T. (2013). Decomposer communities in human-impacted streams: Species dominance rather than richness affects leaf decomposition. *Journal of Applied Ecology*, *50*(5), 1142–1151. https://doi.org/10.1111/1365-2664.12138

Tut, G., Magan, N., Brain, P., & Xu, X. (2021). Molecular Assay Development to Monitor the Kinetics of Viable Populations of Two Biocontrol Agents, *Bacillus subtilis* QST 713 and *Gliocladium catenulatum* J1446, in the Phyllosphere of Lettuce Leaves. *Biology*, *10*(3), 224. https://doi.org/10.3390/biology10030224

Urbaniak, C., Sielaff, A. C., Frey, K. G., Allen, J. E., Singh, N., Jaing, C., Wheeler, K., & Venkateswaran, K. (2018). Detection of antimicrobial resistance genes associated with the International Space Station environmental surfaces. *Scientific Reports*, *8*(1), 814. https://doi.org/10.1038/s41598-017-18506-4

Wang, Q., Liang, J., Zhang, S., Yoza, B. A., Li, Q. X., Zhan, Y., Ye, H., Zhao, P., & Chen, C. (2020). Characteristics of bacterial populations in an industrial scale petrochemical wastewater treatment plant: Composition, function and their association with environmental factors. *Environmental Research*, *189*, 109939. https://doi.org/10.1016/j.envres.2020.109939

Williams, G. J., Denyer, S. P., Hosein, I. K., Hill, D. W., & Maillard, J.-Y. (2007). The development of a new three-step protocol to determine the efficacy of disinfectant wipes on surfaces contaminated with *Staphylococcus aureus*. *Journal of Hospital Infection*, *67*(4), 329–335. https://doi.org/10.1016/j.jhin.2007.08.012

Xie, X., Wang, S., Jiang, S. C., Bahnemann, J., & Hoffmann, M. R. (2016). Sunlight-Activated Propidium Monoazide Pretreatment for Differentiation of Viable and Dead Bacteria by

Quantitative Real-Time Polymerase Chain Reaction. *Environmental Science & Technology Letters*, *3*(2), 57–61. https://doi.org/10.1021/acs.estlett.5b00348

Yang, X., Li, S., Song, G., Xu, X., & Hu, D. (2021). Microbial diversity formed and maintained through substrate feedback regulation and delayed responses induced by Low-Dose Ionizing Radiation. *Acta Astronautica*, *188*, 239–251. https://doi.org/10.1016/j.actaastro.2021.07.027

Yang, X., Xu, X., & Hu, D. (2020). Succession mechanism of microbial community with high species diversity in nutrient-deficient environments with low-dose ionizing radiation. *Ecological Modelling*, *435*, 109270. https://doi.org/10.1016/j.ecolmodel.2020.109270

Zea, L., Prasad, N., Levy, S. E., Stodieck, L., Jones, A., Shrestha, S., & Klaus, D. (2016). A Molecular Genetic Basis Explaining Altered Bacterial Behavior in Space. *PLOS ONE*, *11*(11), e0164359. https://doi.org/10.1371/journal.pone.0164359

Zeng, X.-Y., Li, S.-W., Leng, Y., & Kang, X.-H. (2020). Structural and functional responses of bacterial and fungal communities to multiple heavy metal exposure in arid loess. *Science of The Total Environment*, *723*, 138081. https://doi.org/10.1016/j.scitotenv.2020.138081

Zhang, C., Cui, F., Zeng, G., Jiang, M., Yang, Z., Yu, Z., Zhu, M., & Shen, L. (2015). Quaternary ammonium compounds (QACs): A review on occurrence, fate and toxicity in the environment. *Science of The Total Environment*, *518–519*, 352–362. https://doi.org/10.1016/j.scitotenv.2015.03.007

Zhou, J., & Ning, D. (2017). Stochastic community assembly: Does it matter in microbial ecology? *Microbiology and Molecular Biology Reviews*, *81*(4), e00002-17.

Figures

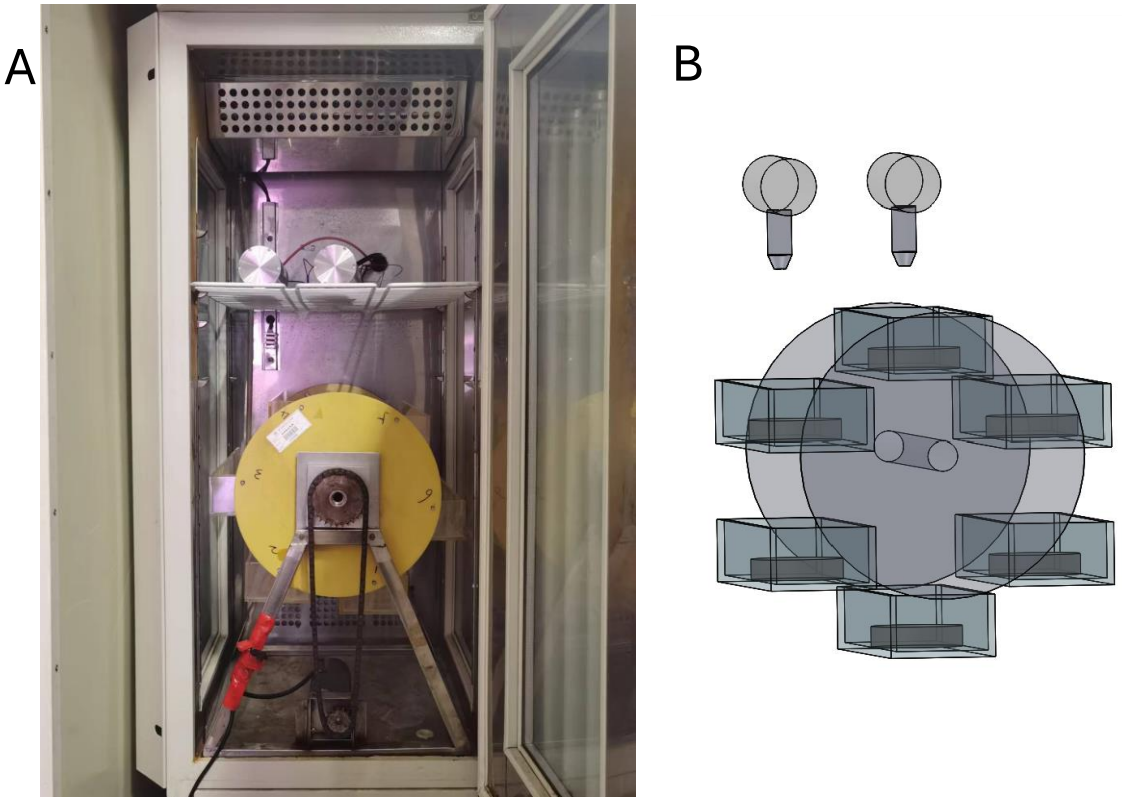

Figure 1: The LDIR environmental simulator (A) and its 3D geometric configuration (B).

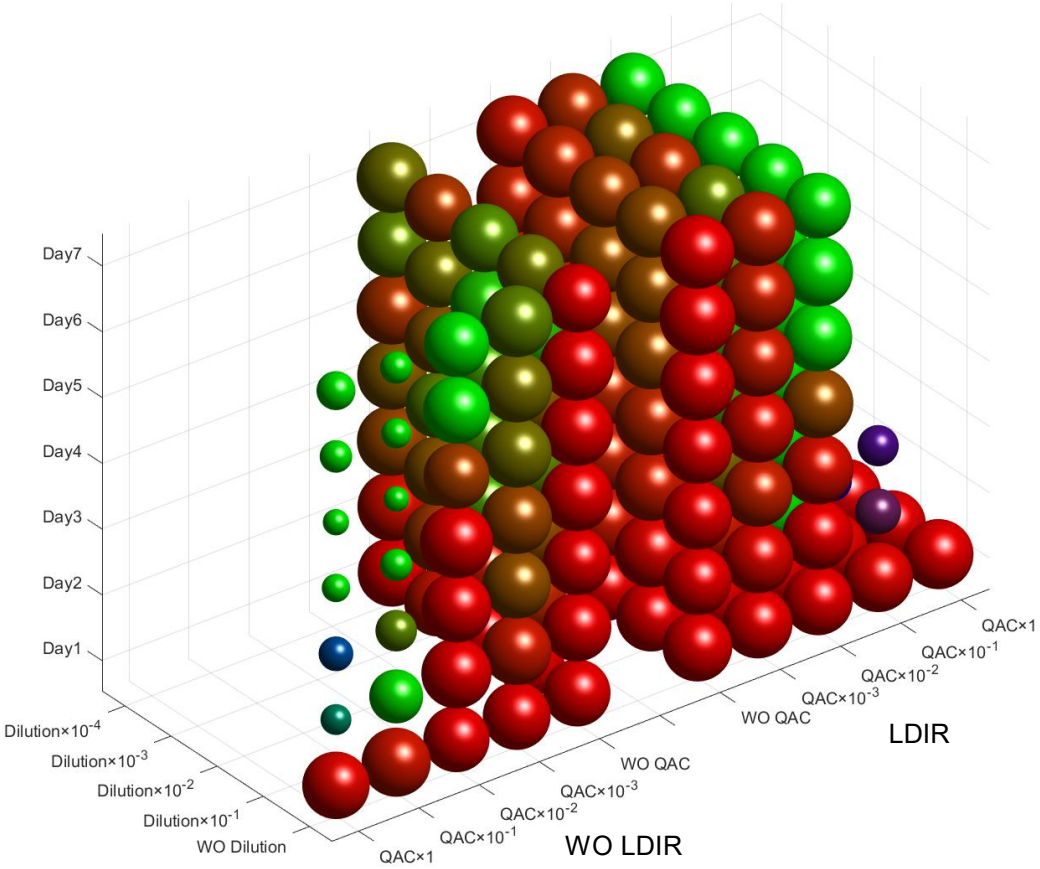

Figure 2: The overview of the community succession under all treatments. The x-axis represents the QAC concentration (e.g. 1 stands for 100%, 10^{-1} stands for 10%), where the left side of axis includes groups without LDIR and the right side includes groups with LDIR; y-axis represents the dilution ratio (e.g. 10^{-1} stands for 10%, 10^{-2} stands for 1%). each position on the x-y plane corresponds to a different treatment. z-axis denotes the number of days, and the seven spheres in each cluster mean seven days of community succession for a treatment group. The radius of the spheres indicates the total biomass in the community (compared to the maximum value and taken as log ten). RGB color shows the percentage of different species (Blue, red and green stand for *Bacillus subtilis*, *Escherichia coli* and *Pseudomonas aeruginosa*, respectively). WO means "without". The 3D version is uploaded as a .fig file in the supplementary materials.

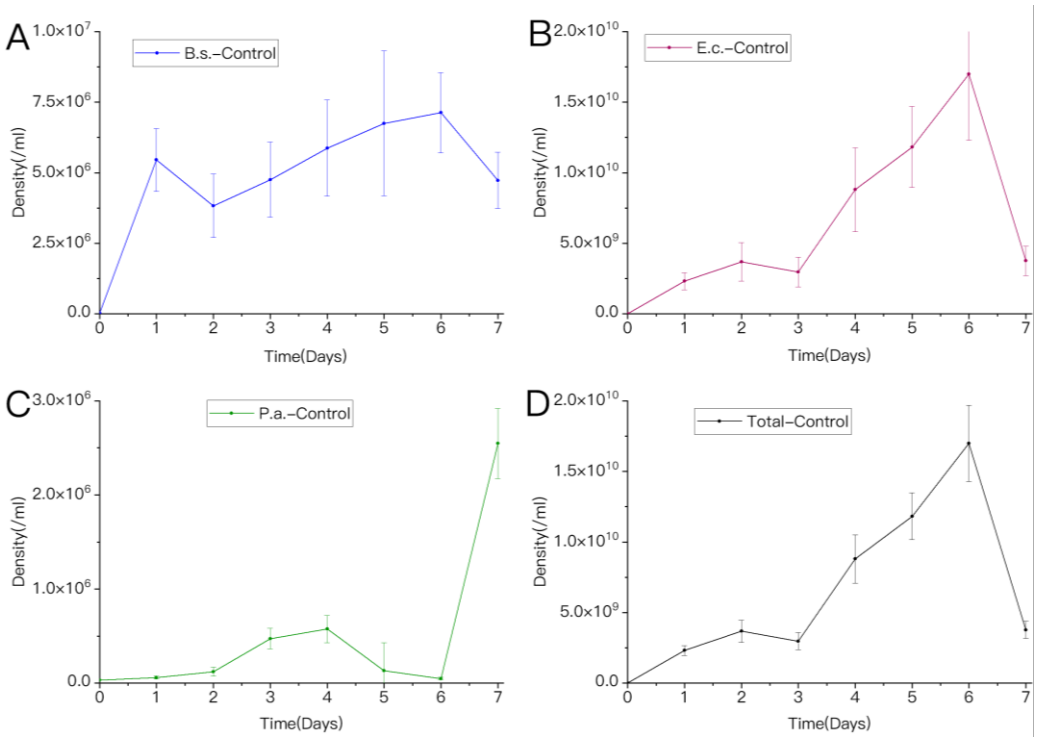

Figure 3: The absolute abundance of three species (A-C) and the total biomass (D) in the control group.

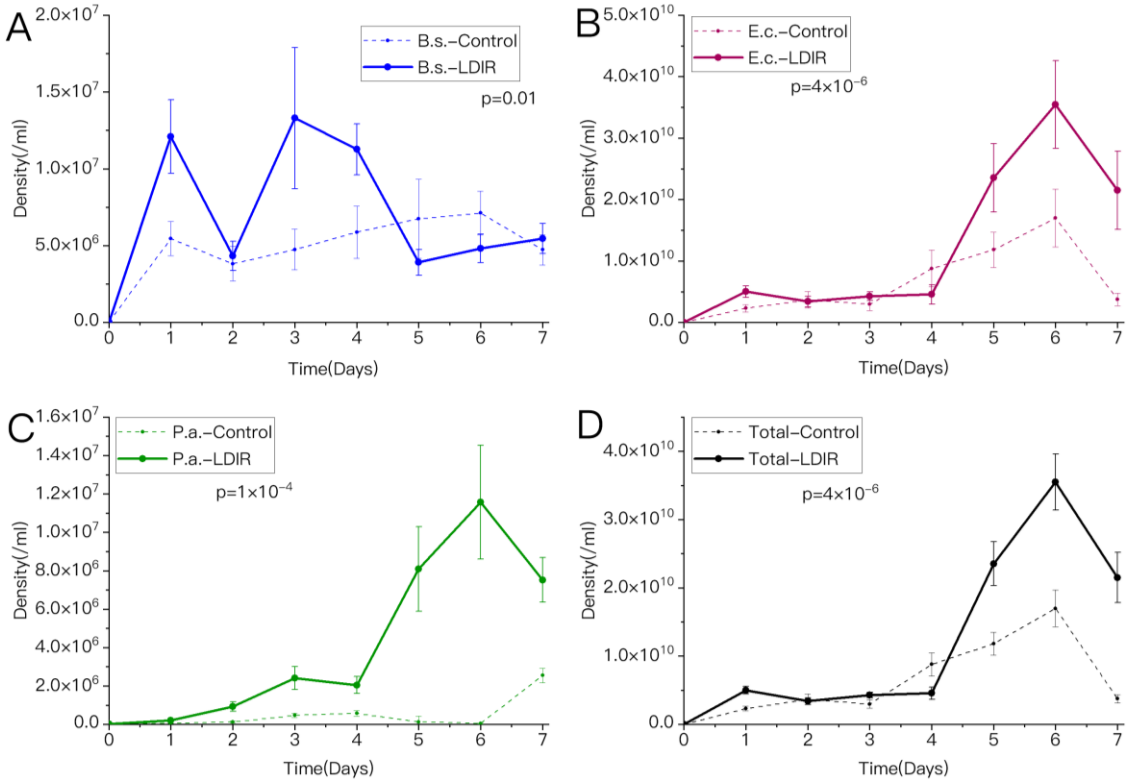

Figure 4: The absolute abundance of three species (A-C) and the total biomass (D) under LDIR (solid line) and in the control group (dotted line).

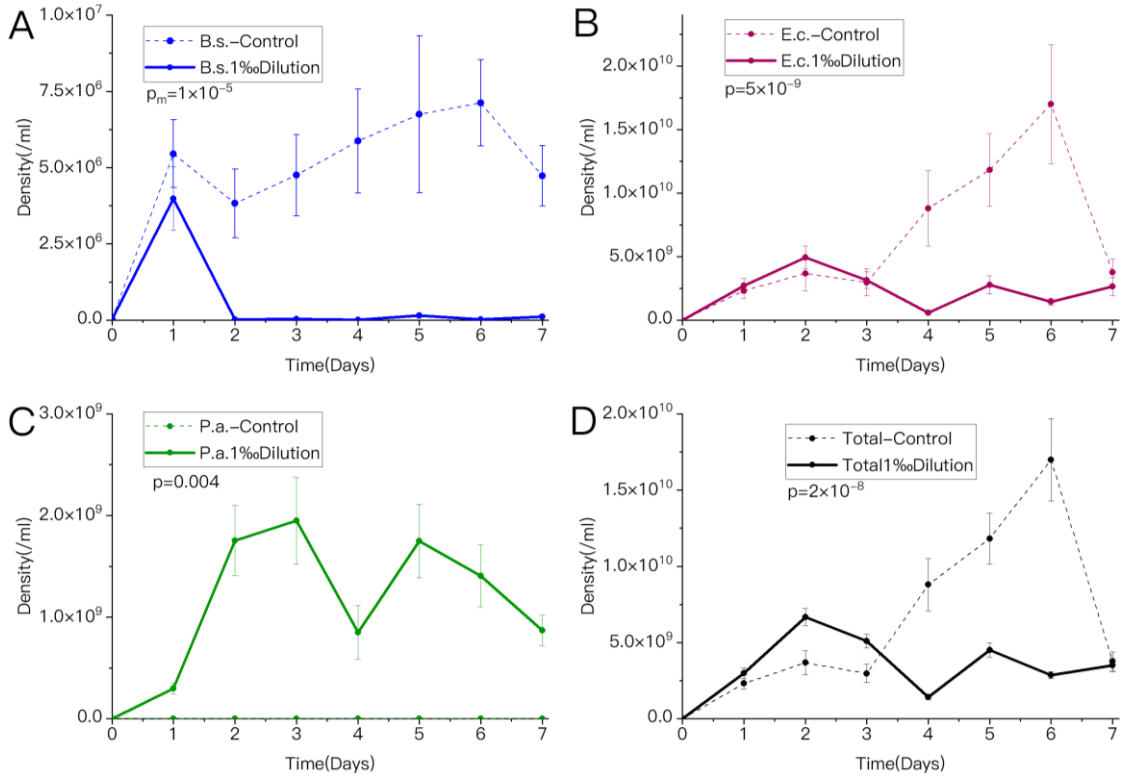

Figure 5: The absolute abundance of three species (A-C) and the total biomass (D) under 1‰ dilution (solid line) and in the control group (dotted line).

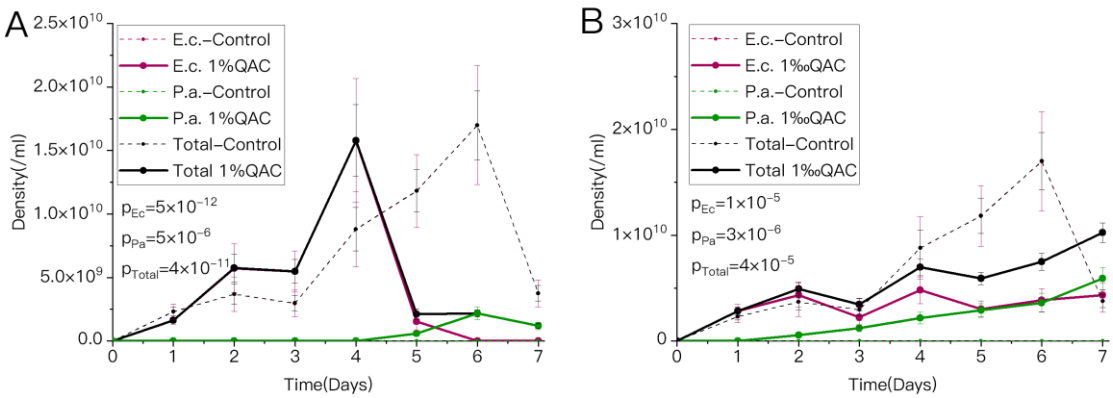

Figure 6: The absolute abundance of *E. coli*, *P. aeruginosa* as well as the total biomass under 1% QAC (A, solid line) and 1‰ QAC (B, solid line) and in the control group (dotted line). *B. subtilis* has a very low abundance, so it is not shown in the figure; the same as below.

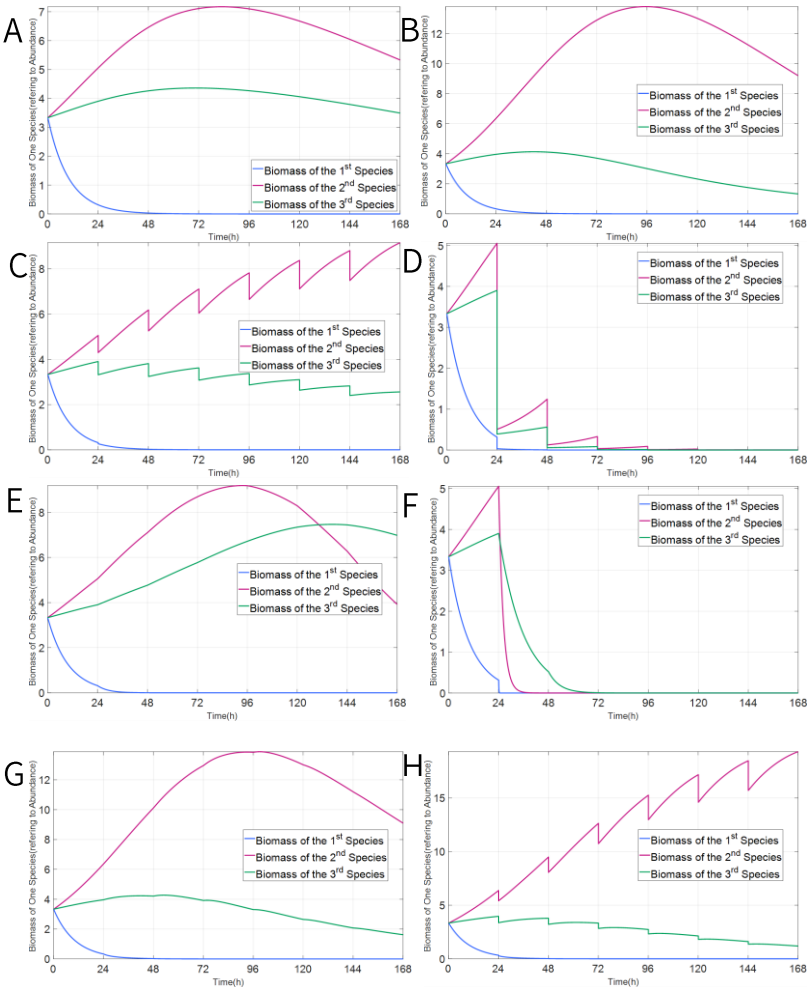

Figure 7: The simulation results from the model built in MatLab/Simulink. A-H represent the control group, LDIR, low dilution rate, high dilution rate, low QAC

concentration, high QAC concentration, LDIR with low QAC concentration, all three factors together, respectively.

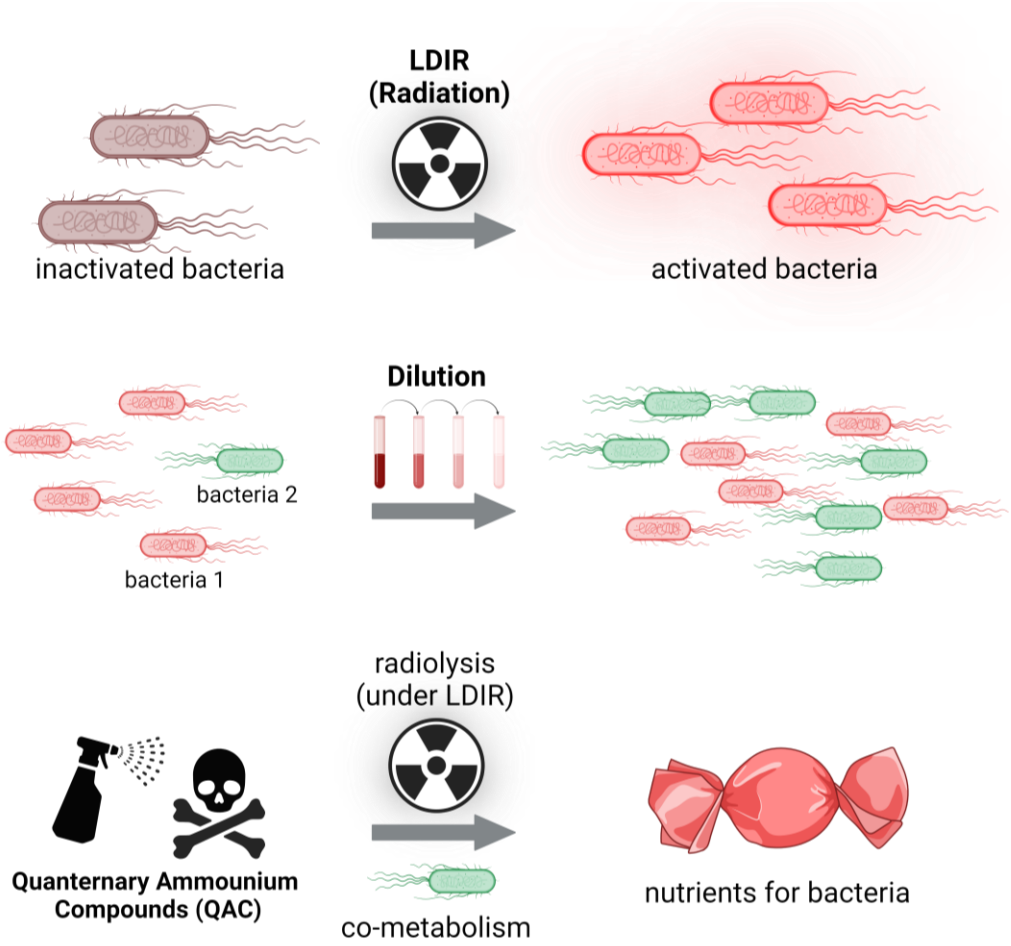

Figure 8: The overall mechanisms of LDIR, dilution and QAC on microbial community succession. LDIR activates all species' growth and reproduction. Dilution allows specific species to be selectively released from suppression. Low-concentration QAC undergoes radiolysis under LDIR and co-metabolism by bacteria, thus changing from bactericide with harmful effects to nutrients. This figure is created with BioRender.com.

Tables

Table 1 Conditions of Distinct Groups

Group	LDIR	Dilution	QAC
1	N	N	N
2	N	10%	N
3	N	1%	N
4	N	1‰	N
5	N	0.1‰	N
6	N	N	100%
7	N	N	10%
8	N	N	1%
9	N	N	1‰
10	Y	N	N
11	Y	10%	N
12	Y	1%	N
13	Y	1‰	N
14	Y	0.1‰	N
15	Y	N	100%
16	Y	10%	100%
17	Y	1%	100%
18	Y	1‰	100%
19	Y	0.1‰	100%
20	Y	N	10%
21	Y	10%	10%
22	Y	1%	10%

23	Y	1‰	10%
24	Y	0.1‰	10%
25	Y	N	1%
26	Y	10%	1%
27	Y	1%	1%
28	Y	1‰	1%
29	Y	0.1‰	1%
30	Y	N	1‰
31	Y	10%	1‰
32	Y	1%	1‰
33	Y	1‰	1‰
34	Y	0.1‰	1‰

"N" means this condition was not applicable in this group. The ratio of dilution meant that part of the culture from t-th day was taken into the R2A solution for gaining the 10ml new culture of $t+1$-th day. No dilution meant that R2A solution was added into the old culture to gain the 10ml new culture. The ratio of QAC meant the stock solution of QAC was added into the culture to make that concentration of the stock solution of QAC.

Table 2 The composition of QAC

Component	per 100ml	Final Concentration
Octyl Decyl Dimethyl Ammonium Chloride (Purity: 80%)	0.5g	0.04%
Dioctyl Dimethyl Ammonium Chloride (Purity: 80%)	0.25g	0.02%
Didecyl Dimethyl Ammonium Chloride (Purity: 95%)	0.21g	0.02%
Alkyl Dimethyl Benzyl Ammonium Chloride, (50% C14, 40% C12, 10% C16) (Purity: 80%)	0.66g	0.0532%

ddH_2O	98ml	-

870 **Table 3 The experimental conditions of distinct metabolomics test series**

Series	LDIR	Dilution	QAC	Day
A	N	N	N	1
B	N	N	N	4
C	N	N	N	5
D	N	N	N	6
E	N	N	N	7
F	N	1‰	N	4
G	N	N	1%	4
H	N	N	1%	5
I	N	N	1%	6
J	N	N	1‰	4
K	N	N	1‰	7
L	Y	N	N	1
M	Y	N	N	4
N	Y	N	N	5
O	Y	N	N	6
P	Y	N	N	7
Q	Y	1‰	N	4
R	Y	N	1%	4
S	Y	N	1%	5
T	Y	N	1%	6
U	Y	1‰	1%	4
V	Y	N	1‰	4

W	Y	N	1‰	7
X	Y	1‰	1‰	4

Supplementary Materials

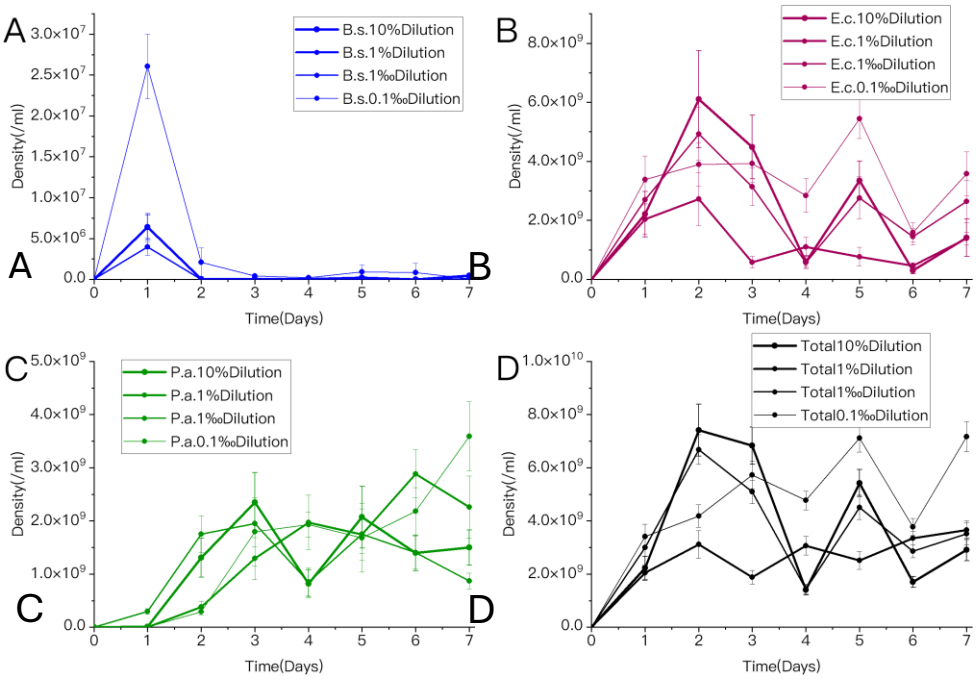

Figure S1: The absolute abundance of three species (A-C) and the total biomass (D) under different dilution ratios. The thinner the line, the more diluted the community in the group is.

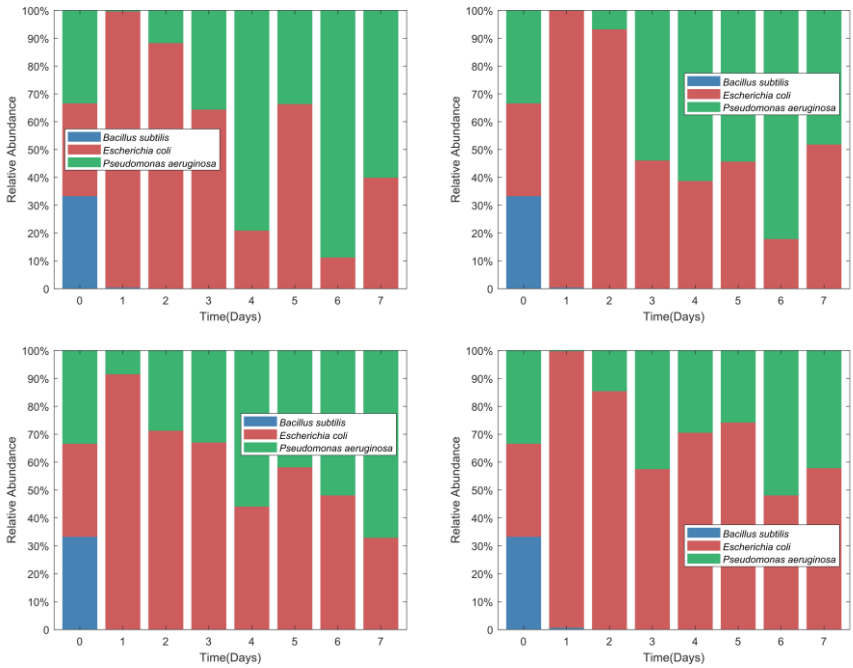

Figure S2: The relative abundance of three species under different dilution ratios. A-D represent 10%, 1%, 1‰ and 0.1‰ dilution ratios, respectively.

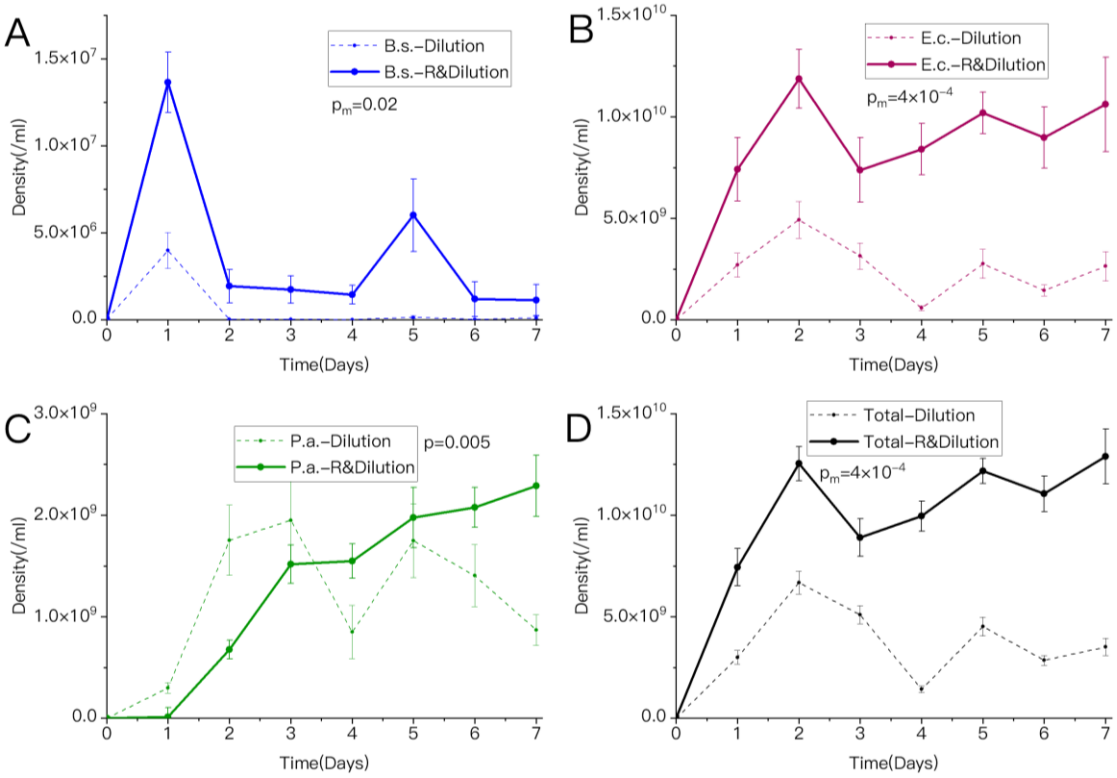

Figure S3: The absolute abundance of three species (A-C) and the total biomass (D) under LDIR and 1‰ dilution (solid line) as well as only 1‰ dilution (dotted line).

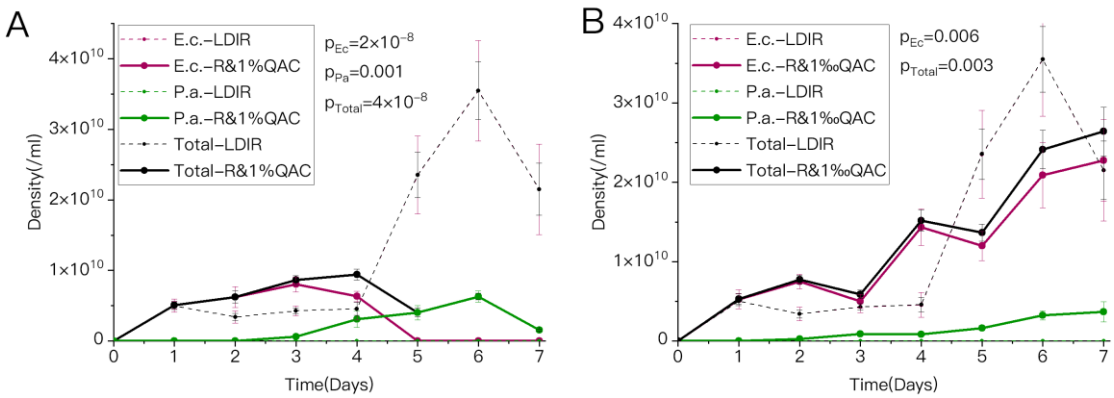

Figure S4: The absolute abundance of *E. coli*, *P. aeruginosa* as well as the total biomass under LDIR and 1% QAC (A, solid line) or LDIR and 1‰ QAC (B, solid line) as well as only LDIR (dotted line).

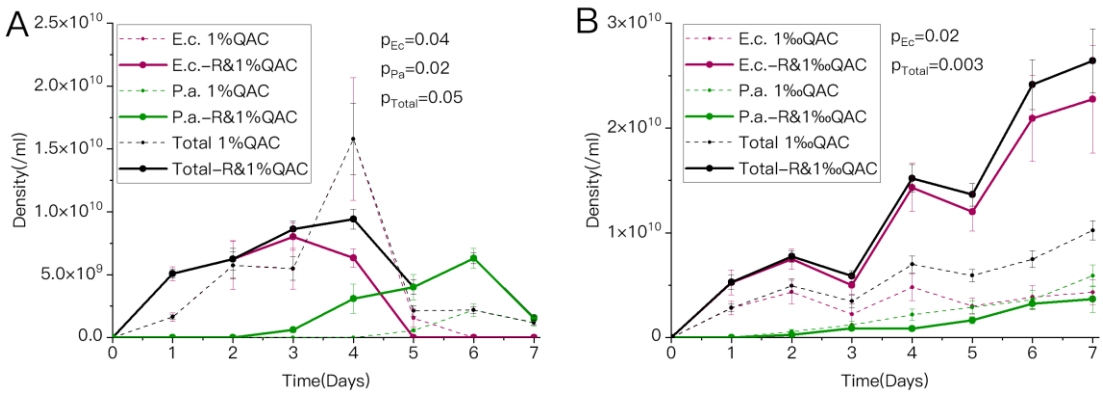

Figure S5: The absolute abundance of *E. coli*, *P. aeruginosa* as well as the total biomass under LDIR and 1% QAC (A, solid line) or LDIR and 1‰ QAC (B, solid line) as well as only 1% QAC (A, dotted line) or 1‰ QAC (B, dotted line).

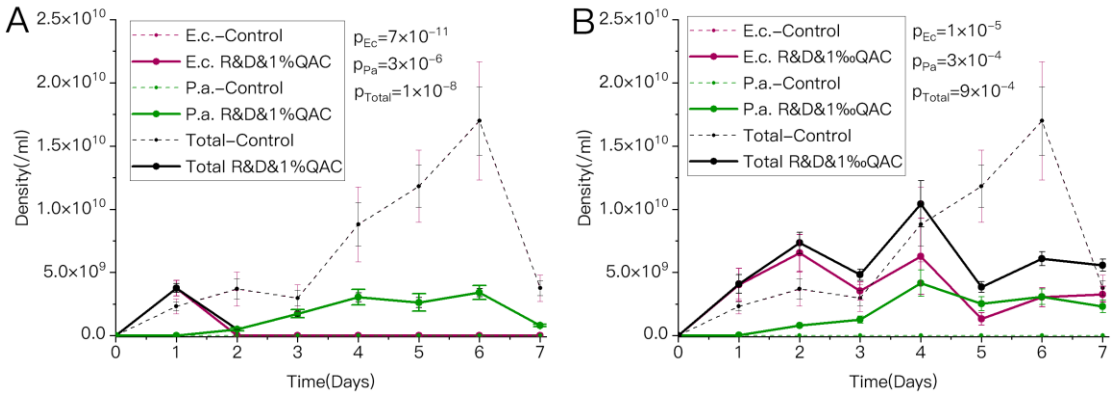

Figure S6: The absolute abundance of *E. coli*, *P. aeruginosa* as well as the total biomass under LDIR, 1% dilution and 1% QAC (A, solid line) or LDIR, 1% dilution and 1‰ QAC (B, solid line) as well as in the control group (dotted line).

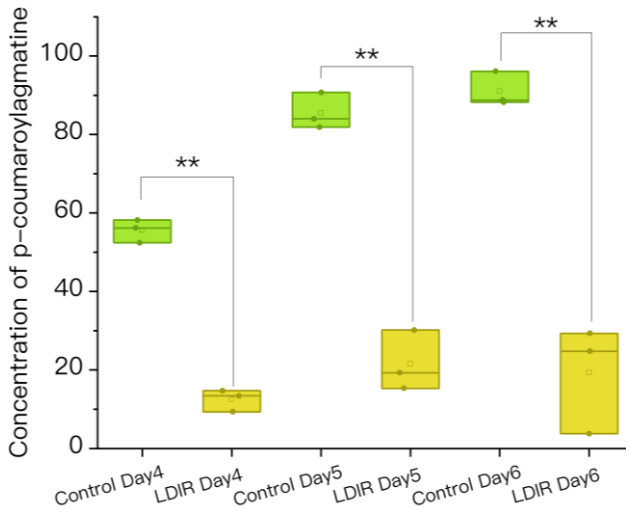

Figure S7: the concentration of p-coumaroyl agmatine in the group exposed under LDIR between the 4-6th days dropped significantly compared with the control

group. "**" meant (p <0.01).

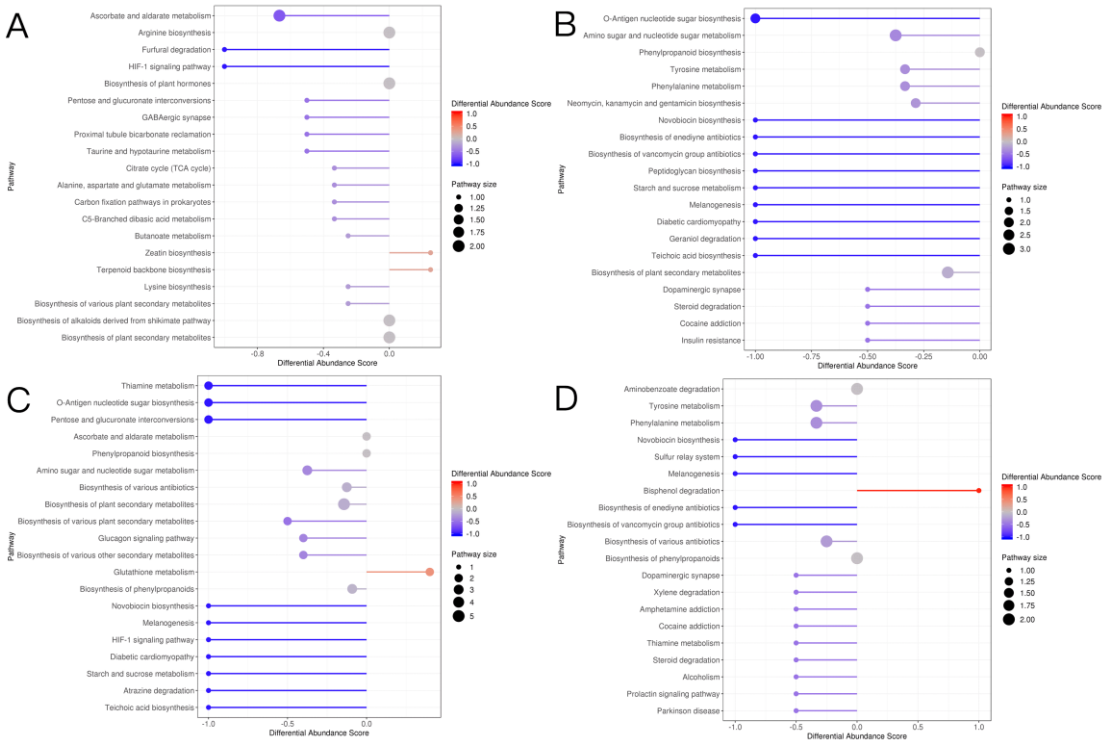

Figure S8: the differential abundance scores of differential metabolisms between the group under LDIR and the control group. A-D represent the 1, 4, 5, 6th day, respectively.

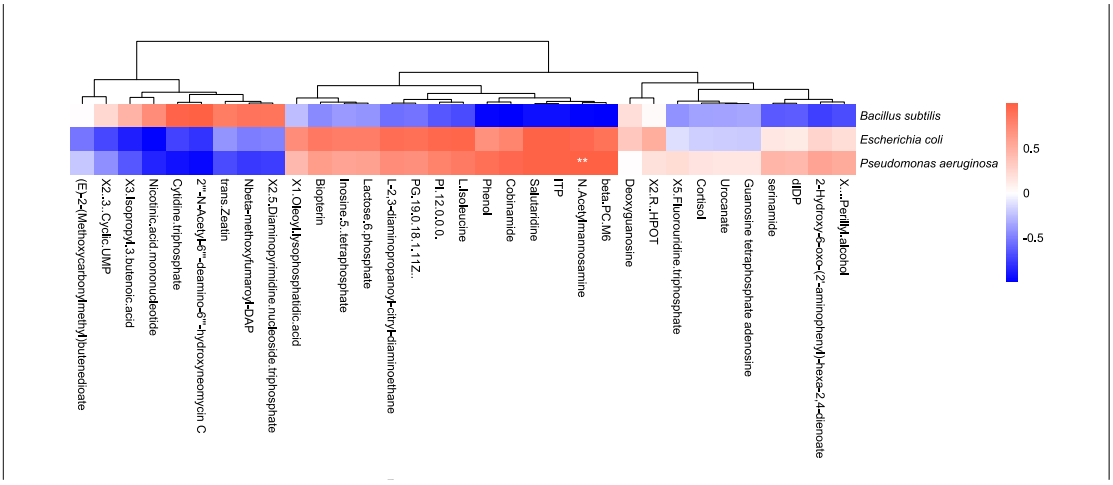

Figure S9: the enrichment of N-acetylmannosamine was markedly correlated with the rise of the abundance of *P. aeruginosa* (p <0.01) on the 4th day of the group diluted with 1‰ ratio per day, compared with the control group. Metabolites with the top 10 highest concentrations in either group, or whose $|\log_2 \mathrm{FC}| \geq 20$ were

considered in the intergroup correlation analysis. "**" meant ($p < 0.01$), and "*" meant ($p < 0.05$). The same is as below.

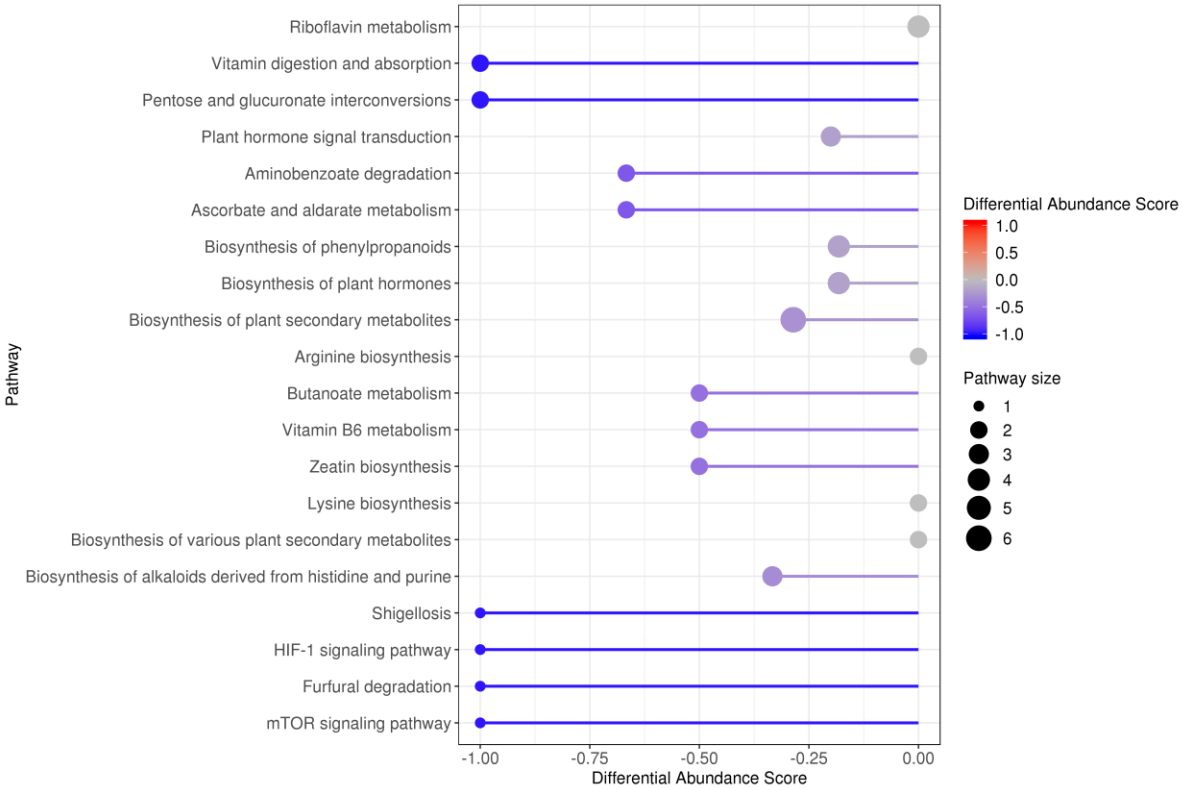

Figure S10: the differential abundance scores of differential metabolisms on 4th day between the group diluted with 1‰ ratio per day and the control group.

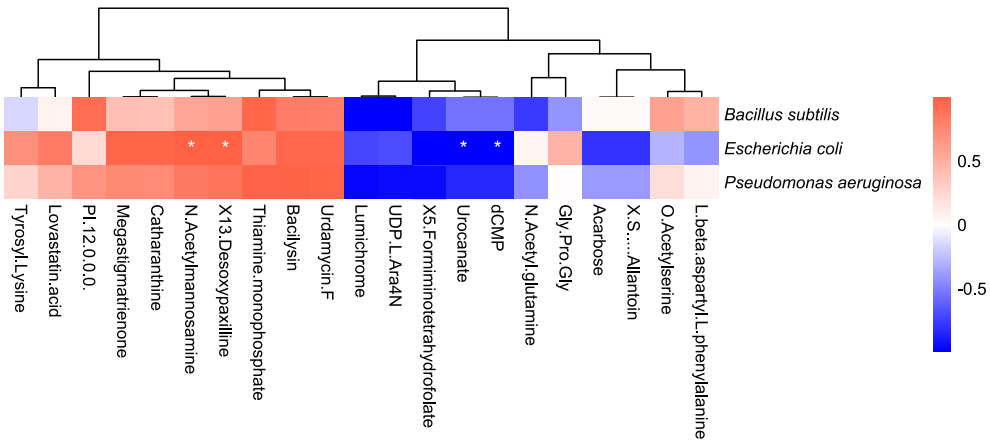

Figure S11: the enrichment of N-acetylmannosamine was markedly correlated with the rise of the abundance of *E. coli* ($p < 0.05$) on the 4th day of the group with 1% stock solution of QAC, compared with the control group.

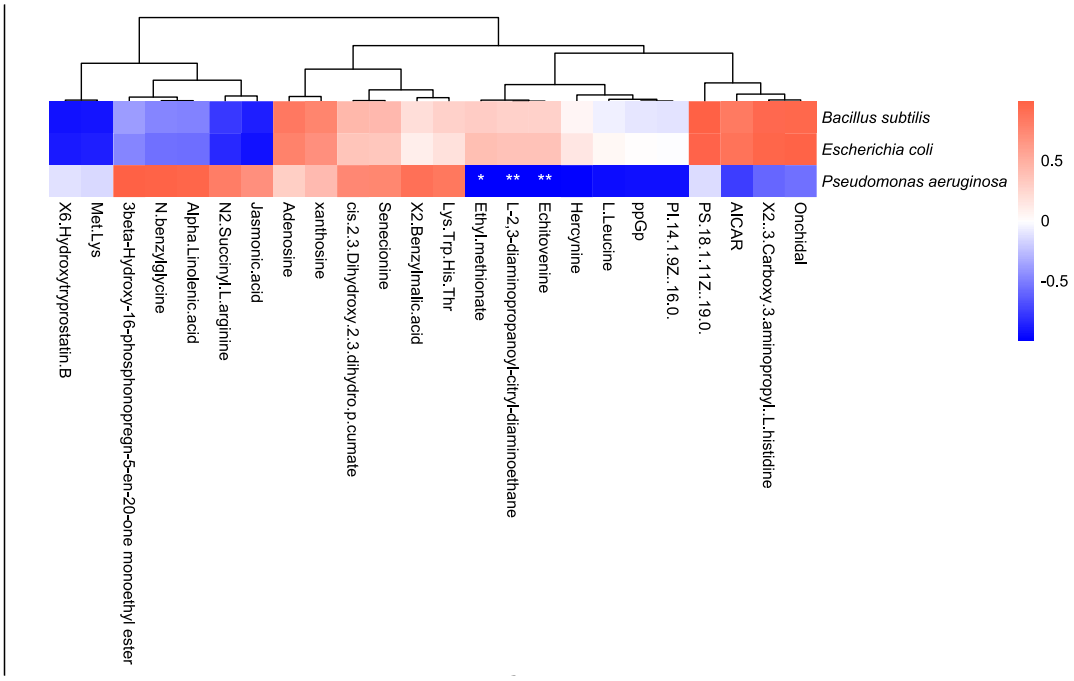

908 **Figure S12: the drop of echitovenine was markedly correlated with the increase of**

909 **the abundance of *P. aeruginosa* ($p < 0.01$) on the 7th day of the group with 1‰**

910 **stock solution of QAC, compared with the control group.**

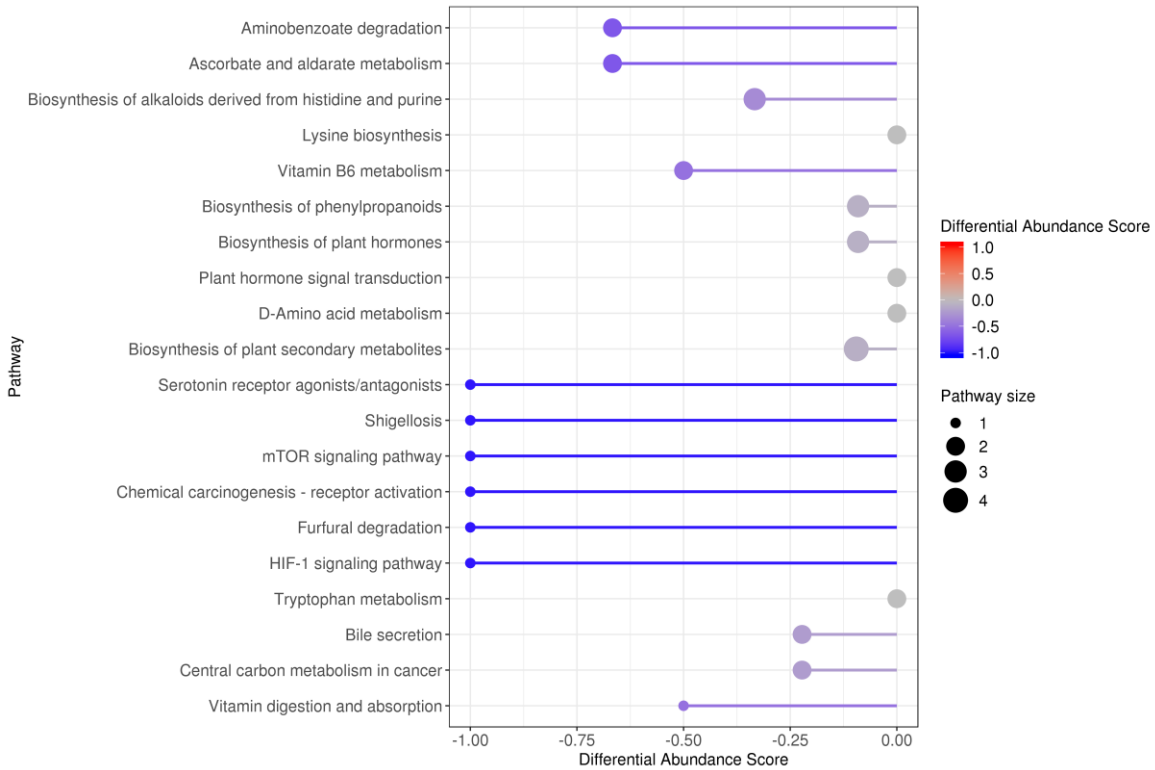

911 **Figure S13: the differential abundance scores of differential metabolisms on 7th**

912 **day between the group with 1‰ stock solution of QAC and the control group.**

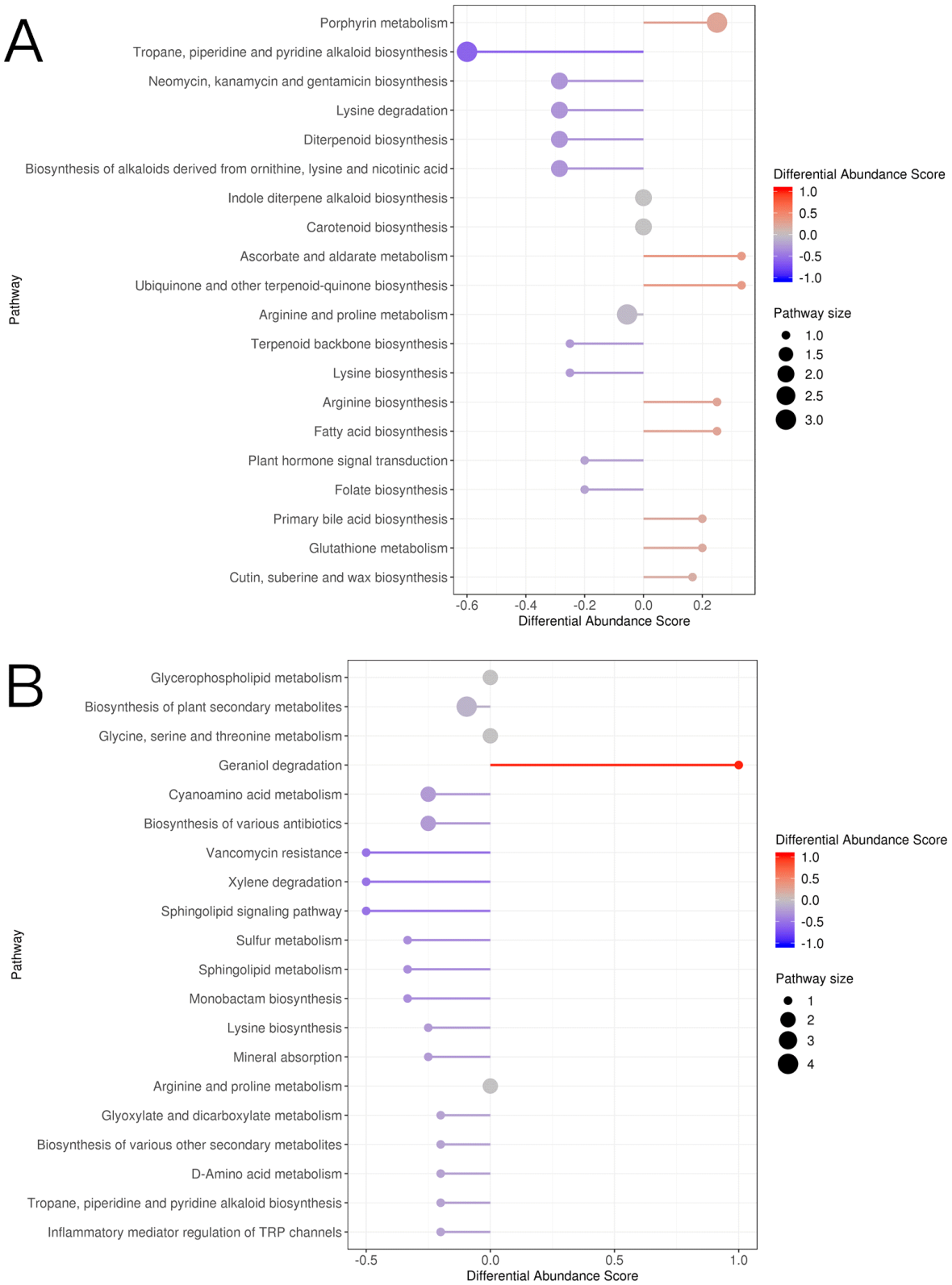

Figure S14: the differential abundance scores of differential metabolisms between the group with both LDIR and 1% stock solution of QAC and the group under 1% stock solution of QAC. A and B represent the 5th and 6th day, separately.

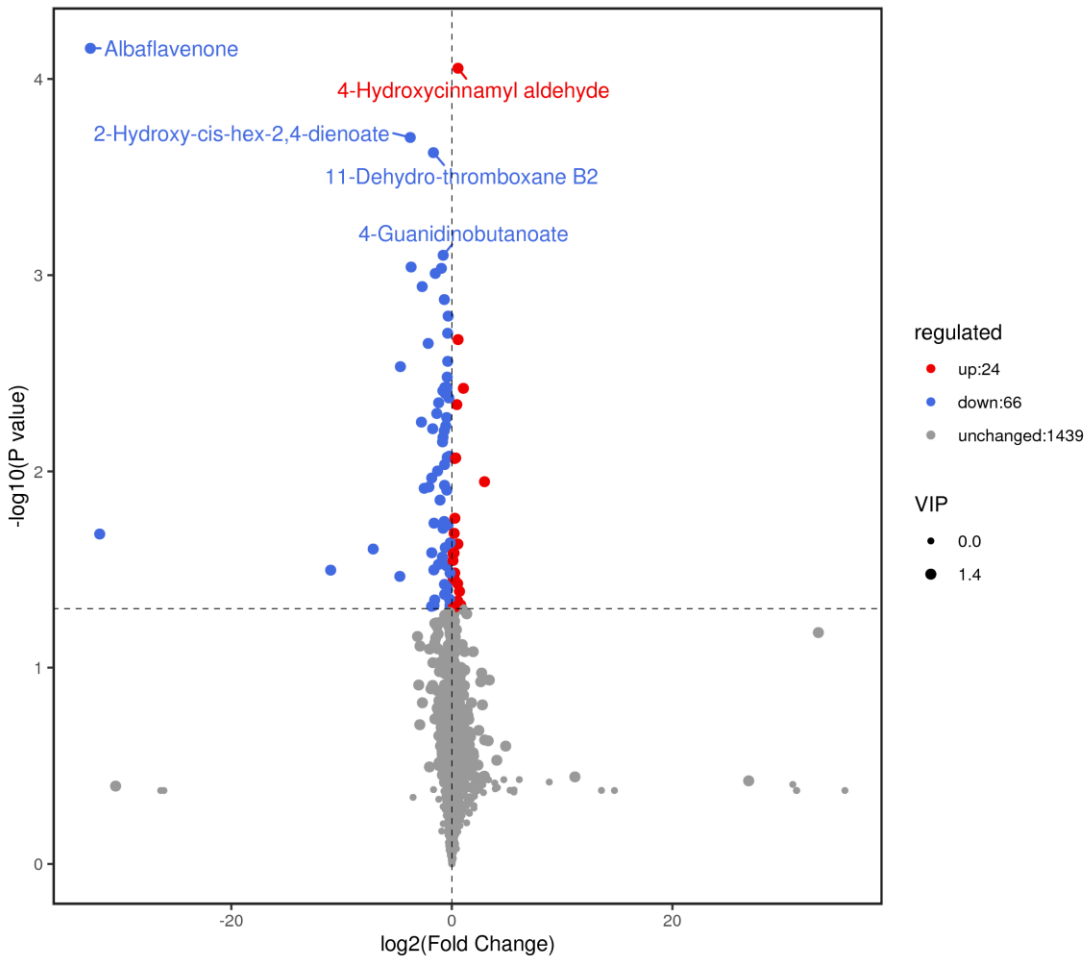

Figure S15: the concentration of albaflavenone sharply diminished on 4th day in the group with both LDIR and 1‰ stock solution of QAC, compared with the control group.

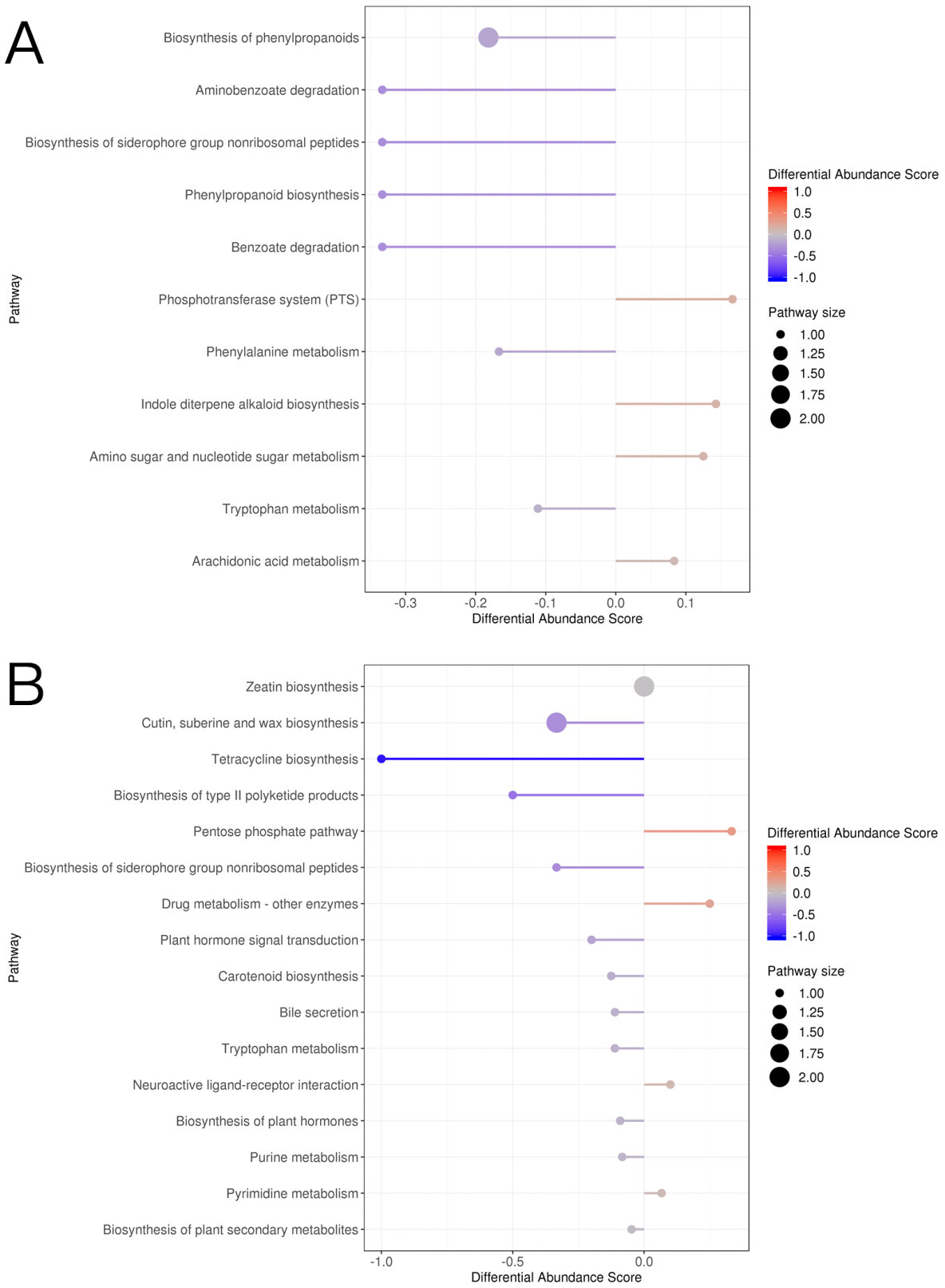

Figure S16: the differential abundance scores of differential metabolisms between the group with both LDIR and 1‰ stock solution of QAC and the group under 1‰ stock solution of QAC. A and B represent the 4th and 7th day, separately.

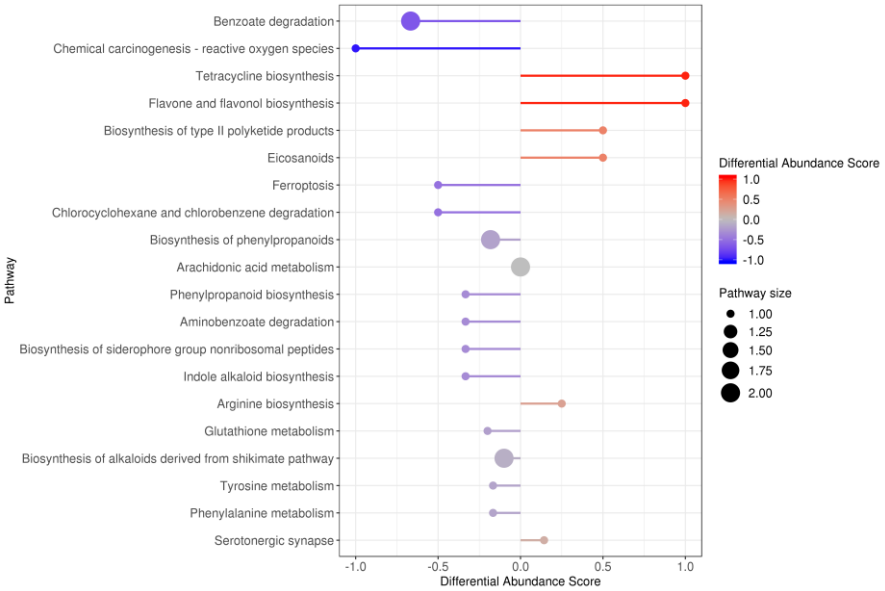

Figure S17: the differential abundance scores of differential metabolisms on 4th day between the groups with 1% stock solution of QAC and 1‰ stock solution of QAC.

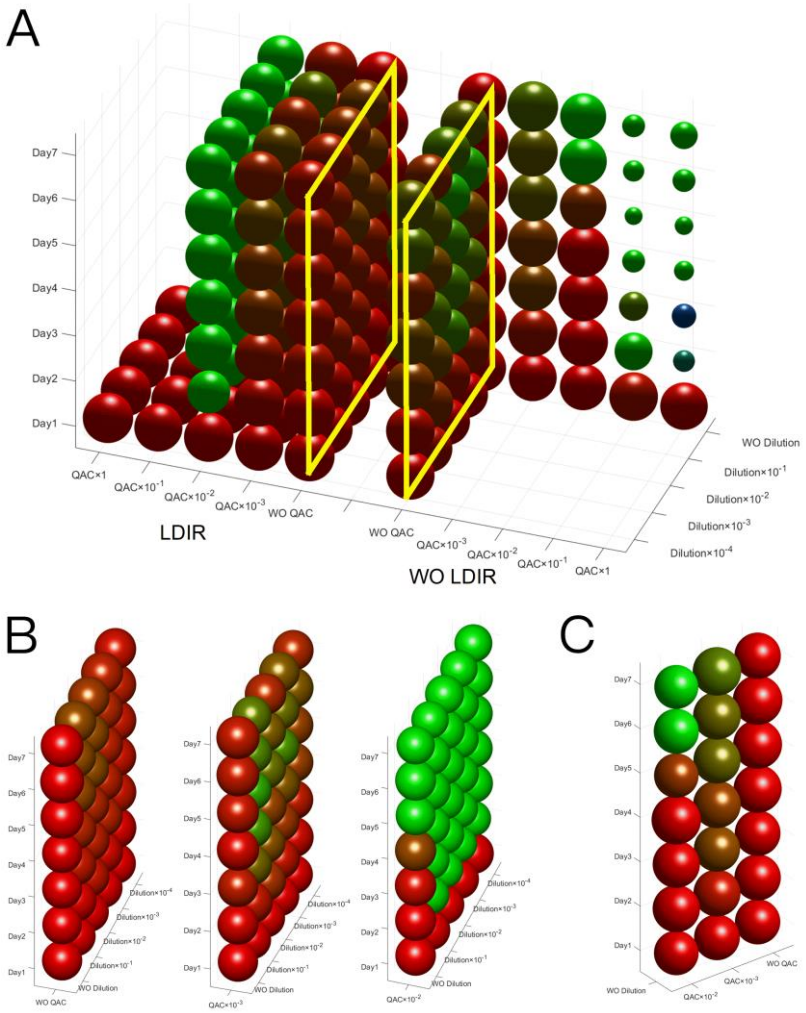

Figure S18: The overview of the community succession under all treatments and its slides. (A) The two planes in the yellow boxes showed that *E.coli* took the majority when both dilution and LDIR were applied compared to only dilution. (B) With higher gradients of QAC under 1%, *P. aeruginosa* gradually became the dominant species with LDIR. (C) With higher gradients of QAC under 1%, *P. aeruginosa* gradually became the dominant species without LDIR.

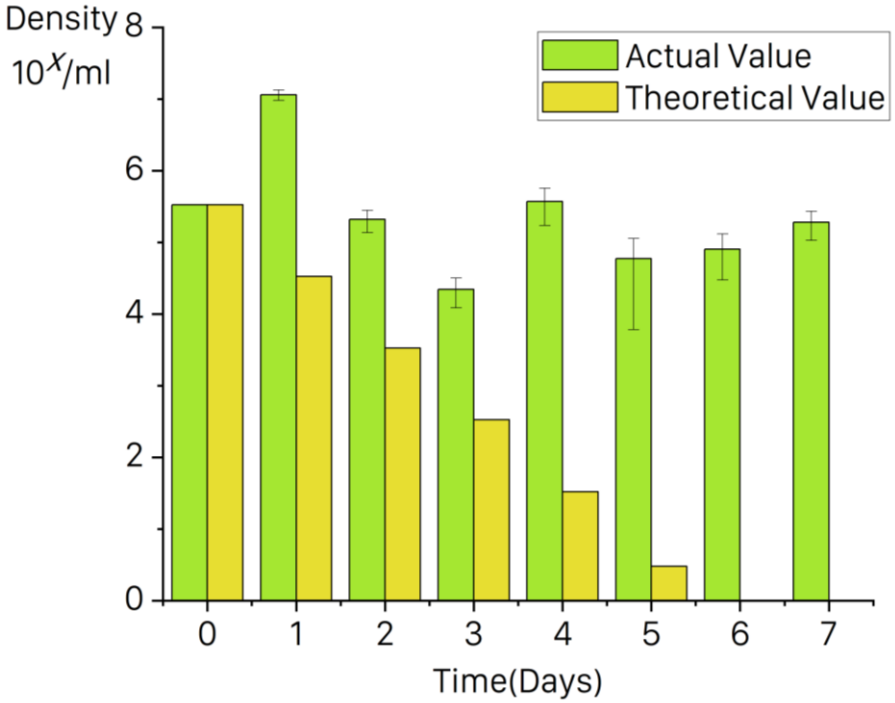

Figure S19: the actual and theoretical counts for 10× gradient dilution of *B. subtilis* cells.

Table S1: The composition of modified minimal R2A

Component	per 1000ml	Final concentration
NaCl	18.0g	1.8%
Peptone	0.5g	0.05%
Yeast Extract Powder	0.5g	0.05%
Casein Peptone	0.5g	0.05%
Sodium Pyruvate	0.3g	0.03%

ddH_2O	1000ml

Table S2 Orthogonal Experiments for PMA-qPCR Conditions

No	PMA Concentration (mmol/L)	PMA Incubation Time (min)	PMA Incubation Temperature (℃)	Light Exposure Time (min)	Light Exposure Temperature (℃)	Light Intensity (W)	Changing Tubes or not	ΔCt(L)	ΔCt(D)
1	50(B)	10	20(A)	30(B)	4(A)	120(B)	N(B)	-0.642	-12.604
2	25(A)	10(A)	37(B)	15(A)	20(B)	120	N	1.845	-8.208
3	25	10	20	15	4	60(A)	Y(A)	-0.712	-14.497
4	50	10	37	30	20	60	Y	0.468	-11.381
5	50	30(B)	37	15	4	60	N	1.614	-15.257
6	25	30	20	30	20	60	N	0.772	-9.731
7	50	30	20	15	20	120	Y	-0.592	-17.972
8	25	30	37	30	4	120	Y	0.17	-10.692
TL_A	2.075	0.959	-1.174*	2.155	0.43*	2.142	-0.666*		
TD_A	-43.128	-46.69	-54.804*	-38.779	-53.05*	-50.866	-54.542*		
TL_B	0.848 (p=0.092)	1.964	4.097	0.768 (p=0.059)	2.493	0.781 (p=0.063)	3.589		
TD_B	-57.214*	-53.652*	-45.538	-44.408*	-47.292	-49.476	-45.8		

ΔCt(L) and ΔCt(D) represent the measured live/dead microbes abundance difference between the control group and experimental group (with PMA), respectively. TL_A and TD_A stand for the sum of the test results ΔCt(L)/ ΔCt(D) for the column with level A, respectively. TL_B and TD_B stand for the sum of the test results ΔCt(L)/ ΔCt(D) for the column with level B, respectively. "*" means $p > 0.05$.

Table S3 Gradient Experiments for PMA-qPCR Conditions

No	PMA Concentration (mmol/L)	PMA Incubation Time	PMA Incubation Temperature	Light Exposure Time	Light Exposure Temperature	Light Intensity (W)	Changing Tubes or not	ΔCt(L)	ΔCt(D)

		(min)	(℃)	(min)	(℃)				
1	50	40	4	30	4	120	Y	0.89	-10.421
2	50	30	20	30	4	120	Y	1.242	-16.583
3	50	10	20	30	4	120	Y	0.244	-13.626
4	50	5	4	30	4	120	Y	0.891	-11.641
5	50	10	4	30	4	120	Y	0.497	-13.451
6	50	30	4	30	4	120	Y	1.045	-18.622
7	50	5	20	30	4	120	Y	1.691	-14.067
8	50	40	20	30	4	120	Y	1.319	-19.609*

Supplementary Material A

Several studies from different perspectives have shown a special phenomenon in *Bacillus subtilis* (Kirchhoff & Cypionka, 2017; Tut et al., 2021; Xie et al., 2016), which is, that some nucleic acid dyes like PMA could penetrate a large number of living cells due to the excessively strong cell membrane potential. Therefore, at the macro level, the rate of false-negative qPCR results would increase, and the threshold for detection of living *Bacillus subtilis* cells through the PMA-qPCR method would spike. In the pre-experiments of this study, *Bacillus subtilis* did not lead in the community. Hence, daily dilution to 10% of the culture yesterday experiment was performed, and the magnitude of counts of *Bacillus subtilis* was much higher than the circumstance "No *Bacillus subtilis* survived, its DNA was diluted simultaneously", as shown in Figure S19. Therefore, direct qPCR was applicable for approximately counting *Bacillus subtilis*.

Supplementary Material B

Eliminating the DNA of dead bacteria cells is the key aim of PMA in PMA-qPCR.

The standard PMA protocol might be suitable for natural environmental samples, but not enough for high-abundance samples, like artificial microbial communities used in this study. Therefore, it is important to optimize its conditions. Related factors included PMA concentration, PMA incubation (with oscillation at 100rpm) time, PMA incubation temperature, light exposure time, light exposure temperature, light intensity (expressed as the blue LED bulb power), whether changing tubes between incubation and light exposure (Banihashemi et al., 2012; Baymiev et al., 2020; Codony et al., 2020; Emerson et al., 2017; Fittipaldi et al., 2012; Fleischmann et al., 2021; Loozen et al., 2011; Martin et al., 2013). To find the highest DNA of dead bacteria cells elimination rate, orthogonal experiments (Table S2) were implemented first on *P. aeruginosa* to screen the better condition of the two-level factor (PMA was not applicable for *B. subtilis* as seen in Sup. A and the primer of *E. coli* used for this study had a relatively high detection threshold). Conditions were selected in previous studies (Agustí et al., 2018; Codony et al., 2020; Emerson et al., 2017; Fittipaldi et al., 2012; Fleischmann et al., 2021; Kralik et al., 2010).

The larger the absolute value of ΔCt(D), the higher the dead bacteria cells' elimination rate. Based on no significant difference of ΔCt(D), the closer ΔCt(L) to zero, the smaller the influence of PMA on live cells. From the orthogonal experiments, these conditions were significantly better: the PMA concentration was 50 mmol/L, the light exposure time was 30min, the light exposure temperature was 4°C, and changing tubes were applied. 120W light intensity has a p-value of 0.063 so it was also selected.

Incubation time and temperature were tested another time in gradient experiments on *P. aeruginosa* as Table S3. As seen in Table, when the PMA incubation time was 40min and the PMA incubation temperature was 20°C, the absolute value of ΔCt(D) was the largest with a significant difference. Therefore, the optimal condition was: to

incubate with 50mmol/L PMA 100rpm for 40min at 20℃, change a new tube, and expose it under a blue LED bulb still for 30min at 4℃.

When applying this optimal condition to *E. coli*, the ΔCt(D)=-18.268. Compared to the standard condition of PMA protocol, the detective elimination rate of dead *E. coli* surged from 25.976% to 99.999%, and that of *P. aeruginosa* dropped from 25.097% to 99.999%. The optimal condition can fulfill the need to measure high species abundance in this study.

Supplementary Material C

In this study, based on LC-QTOF, the qualitative and quantitative analysis of untargeted metabolomics of 72 samples was carried out. A total of 12,079 peaks were detected, of which 1,529 metabolites were annotated. The RSD ≤ 30% ones accounted for more than 60%, so it could be assumed that QC samples have good reproducibility, the instrument was stable, and the requirements of quality control were met.

In OPLS-DA (Orthogonal Projections to Latent Structures-Discriminant Analysis), all results of the experimental and their corresponding control groups could be completely separated, indicating significant overall changes in metabolites for each condition. In the comparison of groups J and V, the Q2Y < 0.5, thus VIP could not be considered as a screening condition for differential metabolites. Besides the above, Q2Y of all other comparisons > 0.5, indicating that the OPLS-DA model was valid. Permutation tests were performed to check the reliability of the OPLS-DA model. The slopes of Q2Y were positive for all groups except for the comparison of J and V, further supporting that the OPLS-DA model was significant. Most of the blue dots in the scatterplots were located above the red dots, indicating good independence of the OPLS-DA model.

In the following analysis, metabolites with the same trend on consecutive days, $|log_2 FC| \geq 20$ (except for $SD = 0$ to remove the systematic error of the instrument) or ranking top 10 were screened.

Supplementary Material D

D1 S-Function

```
function [sys,x0,str,ts] =lss_with2f(t,x,u,flag, X0,mu, Ks, Kf, beta, alpha, delta, phi,
C_I, C_E,D_I,D_E,ep, h, gamma,I,c)
% ============================
switch flag
    case 0
        [sys,x0,str,ts]=mdlInitializeSizes(X0);
    case 1
        sys=mdlDerivatives(t,x,u,mu, Ks, Kf, beta, alpha, delta, phi, C_I, C_E,
D_I,D_E,ep, h, gamma,I,c);
    case 2
        sys=mdlUpdate(t,x,u);
    case 3
        sys=mdlOutputs(t,x,u);
    case 4
        sys=mdlGetTimeOfNextVarHit(t,x,u);
    case 9
        sys=mdlTerminate(t,x,u);
    otherwise
```

```
            DAStudio.error('Simulink:blocks:unhandledFlag', num2str(flag));
end
% =============================================
function [sys,x0,str,ts]=mdlInitializeSizes(X0)
sizes = simsizes;
sizes.NumContStates    = 6;
sizes.NumDiscStates    = 0;
sizes.NumOutputs       = 6;
sizes.NumInputs        = 0;
sizes.DirFeedthrough = 1;
sizes.NumSampleTimes = 1;
sys = simsizes(sizes);
x0    = X0;
str = [];
ts    = [0 0];
%=======================
function sys=mdlDerivatives(t,x,u,mu, Ks, Kf, beta, alpha, delta, phi, C_I, C_E, D_I,
D_E,ep, h, gamma,I,c)
S=x(4);
E=x(5);
F=x(6);
v1b=mu(1)*x(1)*(S/(Ks(1)+S));
v2b=mu(2)*x(2)*(S/(Ks(2)+S));
v3b=mu(3)*x(3)*(S/(Ks(3)+S));
%=================
```

```
va1=beta(1)*exp(-C_I(1)*I-C_E(1)*E)*x(1)^2;
vr1=alpha(1,2)*exp(-D_I(1,2)*I-D_E(1,2)*E)*x(1)*x(2)+alpha(1,3)*exp(-
D_I(1,3)*I-D_E(1,3)*E)*x(1)*x(3)
vv1=delta(1)*x(1)+ep(1)*x(1)*E;
%=================
va2=beta(2)*exp(-C_I(2)*I-C_E(2)*E)*x(2)^2;
vr2=alpha(2,1)*exp(-D_I(2,1)*I-D_E(2,1)*E)*x(2)*x(1)+alpha(2,3)*exp(-
D_I(2,3)*I-D_E(2,3)*E)*x(2)*x(3);
vv2=delta(2)*x(2)+ep(2)*x(2)*E;
%=================
va3=beta(3)*exp(-C_I(3)*I-C_E(3)*E)*x(3)^2;
vr3=alpha(3,1)*exp(-D_I(3,1)*I-D_E(3,2)*E)*x(3)*x(1)+alpha(3,2)*exp(-
D_I(3,2)*I-D_E(3,2)*E)*x(3)*x(2);
vv3=delta(3)*x(3)+ep(3)*x(3)*E;
%=================
ve=gamma*I*E;
%=================
sys = [v1b-va1-vr1-vv1;...
       v2b-va2-vr2-vv2;...
       v3b-va3-vr3-vv3;...
      h*ve-phi(1)*v1b-phi(2)*v2b-phi(3)*v3b;...
      -ve;...
       h*ve];
%=================
function sys=mdlUpdate(t,x,u)
```

```
sys = [];
%=================
function sys=mdlOutputs(t,x,u)
sys = x(1:6);
%=================
function sys=mdlGetTimeOfNextVarHit(t,x,u)
sys=[];
%=================
function sys=mdlTerminate(t,x,u)
sys = [];
%=================
```

```
D2 Main Function
clear;clc;shg
rng(5);
set_param(gcs,'MaxStep','.08');

S0=50+2*rand;
E0=0;
F0=0;
X0=[3.3333;3.3333;3.3333;S0;E0;F0];
mu=[0.01;0.1;0.045];
Ks=20+rand(3,1);
Kf=0.05+0.005*rand(3,1);
beta=[0.002;0.003;0.001];
alpha=.003*rand(3);
delta=[0.1;0.03;0.015];
phi=rand(3,1);
C_I=1*rand(3,1);
C_E=1*rand(3,1);
D_I=1*rand(3);
D_E=1*rand(3);
h=0.1;
gamma=.1+.2*rand;
I=0;
c=rand(3,1);
t=[];
y=[];
dilution=1;
ep=[0.1;0.005;0.001];
%        ============================
for i=1:7
        lss=sim(gcs,[0,24]);
        t=[t;(lss.tout+24*(i-1)+0.08)];
        y=[y;lss.yout];
        X0(1:3)=dilution*y(end,(1:3));
```

```
        if dilution<1
            X0(4)=S0;
        else
            X0(4)=y(end,4);
        end
        E0=1;
        X0(5)=dilution*y(end,5)+E0;
        X0(6)=dilution*y(end,6);
end
plot(t,y(:,1),'LineStyle','-','Color','#3366FF','linew',3);
hold on
plot(t,y(:,2),'LineStyle','-','Color','#c71585','linew',3);
plot(t,y(:,3),'LineStyle','-','Color','#00a15c','linew',3);
grid
set(gca,'YLim',[0,inf],'XLim',[0,168],'XTickMode','manual','XTick',[0:24:168],'FontSize',30);
legend('Biomass of the 1^s^t Species','Biomass of the 2^n^d Species','Biomass of the 3^r^d Species','location','best','FontSize',30)
xlabel('Time(h)','FontSize',25)
ylabel('Biomass of One Species(refering to Abundance)','FontSize',25)
hold off
```

D3 MatLab/Simulink Block Diagrams

Available on GitHub: https://github.com/angkuLC/codeforcureorcurse.